

We thank the reviewers for their constructive comments. You may find below a point-by-point reply to the reviewer's comments and the marked-up manuscript version.

### **Response to Reviewer #1 comments**

Page 4944. Line 24. Please, update the cite Munich Re Group, 2003 to a more recent one. I would suggest Kundzewicz, Z.W. et al., 2014.

The update was done, good suggestion indeed.

Page 4946. Line 17. Climate and historical floods (add s to flood)

This has been changed.

Page 4949 line 5. I would suggest to change “to represent the river energy” as follow: “to be related with the stream flow energy of the river entering the lake”

This has been changed.

Page 4952, line 10 the term “small gravel” is not correct. Use one of the follow scientific terms accordingly: granular gravel (2 to 4 mm) or pebble gravel (4 to 64 mm).

'small' was changed to 'pebble'.

Page 4953. Line 24. “Relative Ca intensities are most of the time very low “ Is this sentence correct? shouldn't be "Relative Ca content: : :”

This was indeed a mistake. 'Relative' was deleted.

Page 4954. Line 4. I think that (Fig.4) should be (Fig. 3). Please, check.

Yes, this has been changed.

Page 4956. In the sentence “during sliding of slope sediments and then deposited over the debrites” it took me some time to understand that slope sediments are indeed on slope within the lake bed. I don't know if you may say “slope sediments within the lake bed and then: : :”. Otherwise, leave as it is now.

The words “lake bed” are not used by sedimentologists working on lake and may be confusing as well. We added thus the term 'subaquatic' slope sediment for clarity.

Page 4962. Line 7 change to “summer-to-autumn flood events”

This has been changed.

Page 4963. Line 13. Replace the reference Benito et al. 2008 to the latest one: Benito, G., Macklin, M.G., Zielhofer, C., Jones A., and Machado, M.J. (2015). Holocene flooding and climate change in the Mediterranean. Catena 130, 13-33.

The reference has been updated.

Page 4963. Line 15. Delete “and contemporaneous intensification”

This has been changed.

Page 4963. Line 20. The occurrence of a higher frequency of very large floods during the MCA in western Mediterranean is not new, and it was also described in other detail fluvial palaeoflood and historical records such as the Tagus river.

The sentence was modified to specify that this statement concerns the Alpine area:

'In contrary, the occurrence of high-intense floods during both the MCA and the LIA periods is a new feature of Alpine regional patterns, since the most intense floods occurred exclusively during the MCA in the Blanc record (Wilhelm et al., 2013) or during the LIA in the Allos record (Wilhelm et al., 2012a; Fig. 8) and other Mediterranean records of the Alpine region (Jorda and Provansal, 1996; Miramont et al., 1998; Jorda et al., 2002; Arnaud-Fassetta et al., 2010).'

## Response to Reviewer #2 comments

### MAJOR REMARKS:

1) Deposit thickness as proxy for flood intensity: The approximation of flood intensity using the thickness of the deposits does not seem to hold for Lake Foréant. As you indicate on lines 4949-2to7 grain size would be the best proxy for flood intensity. On lines 4953-20to23 and 4959-6to9 you mention that there is no significant grain-size variability that could give an indication on flood intensity, and that you therefore use the deposit thickness as proxy for intensity. As a result, you find that the intensity of the events during the warmer MCA is higher than during the cool LIA (Fig. 8). This is not a legitimate conclusion, as you have no proof (or calibration) showing that deposit thickness is really proportional to flood intensity. During the MCA, floods occur less frequent than during the LIA and a sediment storage effect in the catchment could therefore become highly important. For MCA floods, which occur at longer time intervals, more sediment is thus available for mobilization by the river because the catchment has not been 'emptied' for a longer period of time than during the LIA. In this context, please also see my second-last comment on the discussion part. The study with the fungal spores is helpful for ruling out anthropogenic influences on sediment mobilization, but you still have to take into account natural sedimentary processes acting in the catchment. In my opinion, the thickness of the deposits can therefore not be used as a proxy for flood intensity. As a consequence you would need to adapt the focus of this study ('Frequency and intensity : : :') and text passages referring to intensity. An additional remark regarding the grain-size results: The results are only shown as a small inset in Figure 2, and you mention it shortly on lines 4953-20to23 and 4959-6to9. However, at these positions in the text you do not show or describe your results but you add many references. The effect is that it looks like the grain-size results were published in the indicated references. Instead, I propose that you show the grain-size results more prominent in this paper.

We appreciate this comment of Reviewer 2, as he touches a complex aspect in our study. However, we prefer to stick to the use of thickness as proxy for the following reasons:

1. We did not indicate that grain size may be the 'best' proxy. Actually there is no universal 'best way' but there are only 'site-specific' ways depending on the sedimentary environment of the studied catchment-lake system. Having said this, it is true that there are other means to reconstruct flood intensity, i.e. by assessing the amount of flood-sediment volume, which indeed was not indicated in the 'methods' section. We thus reworked the section 3.2. to clarify i) that two distinct proxies (grain size and flood-sediment volume of flood layers) have been shown by previous works to be relevant to reconstruct flood intensity and ii) that, as a result, these two proxies were explored in our study.
2. Previous studies in Alpine environments (e.g. Wilhelm et al., 2012b; Jenny et al., 2014; Wilhelm et al., 2015) showed through calibrations that the intensity of past floods may be reliably assessed from the flood-layer thickness when i) there is no significant variability of grain size in the flood layers and ii) when the depositional pattern of the flood layers is stable over time. As these conditions were observed in Lake Foréant, we are confident about identification of the high-intense events. These preconditions that make our study reliable are now clearly indicated in section 3.2. and 5.2.
3. Coarse particles (> 100 µm) are transported by processes acting close to the river bed (saltation, rolling, etc.; e.g. Passega, 1964) and, thereby, they are sensitive to a threshold flow velocity below which these coarse particles are deposited (cf. Hjulström curve). In contrast, fine particles (i.e. clays and fine silts that composed the Foréant flood layers) are transported by suspension in the river. As a result, trapping and storage of these particles in the small Foréant alluvial plain is unlikely making flood-layer thickness a meaningful parameter. This is supported by the relatively stable sedimentation rate of the silty sedimentary background deposits (Fig. 6) that suggests an uninterrupted sediment transport to the lake over the studied period. The section 5.2.2. was reworked to clarify this point.

4. The negligible storage effect of fine particles during floods is supported by other studies. For instance, a calibration study of the Lake Le Bourget palaeoflood record showed that the amount of fine particles transported and deposited in a lake during floods is proportional to the river discharge, even in a large catchment area where places for sediment storage are present and dams have been built during the calibration period (Jenny et al., 2014).
5. Grain-size data are used, shown and commented as other results from this study. References have been deleted from the section 'Results' (lines 4953-20to23) to avoid confusion between data of this study and others studies.

2) 'Turbidites', 'debrites' etc: My impression is that the use of the terms 'turbidites, debrites, event layers, and flood deposits' may be a bit confusing and is not consistently used throughout the manuscript. Furthermore, for the MMIT (mass-movement induced turbidite) I do not really agree why you have to separate the deposit into a turbidite and a debrite. Sedimentologically I might understand your aim, but still, it is one single event that leads to the deposition of the debrites and the turbidite on top. So why not simply call the complete deposit MMIT and describe in chapter 4.1 how it is composed. This would leave you with 168 flood deposits and 3 MMITs. Instead of 171 turbidites minus the 3 turbidites belonging to the MMITs. In addition, in the methods section you already speak of event layers (4948-20) that were detected by density anomalies, and of flood deposits (4949-13) that were detected by geochemical data. Is there a difference here between event layers and flood deposits? In section 4.1 you then speak of coarsegrained layers or graded beds or turbidites. In total, this is a bit confusing and I propose that you speak of detrital layers or event layers (if necessary with, for instance, the addition 'coarse-grained' or 'homogeneous') as long as you haven't interpreted the trigger. Afterwards, you can speak of flood deposits and MMITs. The term turbidite: you mention that the grading is very weak in the detrital layers. I am therefore not convinced that the term 'turbidite' is sedimentologically appropriate here. Maybe it would be better to omit the term 'turbidite' and speak of detrital layers or event layers, as outlined above.

We followed the comment of the reviewer to avoid confusion. We deleted the terms 'turbidite' and 'debrite' and only speak of 'event layers' in the method section, 'graded layer' and 'coarse-grained layer' in the result section and, 'mass-movement-induced layer' (MMIL) and 'flood-induced layer' (FIL) in the discussion section. In addition, some parts were reworked to describe the MMILs as the stratigraphic succession of a coarse-grained layer and a graded layer.

3) XRF counts as quantitative indication of element concentrations: You use the low XRF core scanning Ca counts in the sediments as direct indication that Ca concentrations are indeed low compared to the concentration of other elements. XRF core scanning results are qualitative and many factors (e.g. sediment matrix, machine-specific properties) influence the counts. Have you calibrated the results via e.g. ICP-MS? The assumption that the counts are proportional to the element concentrations is speculative, unless you have additional data to show it.

The reviewer's comment is correct in a sense that scanning XRF counts should not be confused with absolute concentrations measured by calibrated quantitative methods. The use of the term 'content' leads to some confusion here. We are well aware of the fact that count rates/intensities derived from scanning XRF are only the reflection of relative/semi-quantitative changes in element intensities, which are mostly driven by changes in element concentration with typically minor bias by changes in sediment matrix (i.e. water content, grain-size, sediment composition). We used the same measurement conditions for all scanning XRF measurements conducted here. Tube aging- a common issue, which needs to be corrected for when using very long integration times or when measuring several 100 m long sediment successions should not be an issue given the comparably short total measurement times used in this study. Machine-specific property changes should not be an issue here. Sediment matrix effects can be a challenge in sediment successions with strong changes in sediment composition- i.e. rapid changes from calcareous to diatomaceous to clastic muds. We conducted a careful reevaluation of every XRF spectra after measurement in order to minimize bias induced by changes in sediment matrix. During reevaluation we found that changes in sediment matrix, in case of the Foreant sediment successions studied here, are very small. This is because changes in sediment composition are rather small- the sediment is primarily composed of detrital clasts with only low

contents of OM, endogenic mineral phases, and siliceous fossils. In addition we only focus on elements that are typically abundant in high concentrations (>1000ppm) and that can easily be measured with the measurement set up we used in our study. Therefore we believe that our approach is far from speculation and that we can use downcore changes in element intensities measured with a state-of-the-art ITRAX XRF Scanner (acquired in 2013) as indicators for semi-quantitative changes in element concentration. In order to minimize confusion we changed the term ‘content(s)’ to ‘intensities’.

#### DETAILED REMARKS:

TITLE According to my point 1 above you might have to adapt.

See response to comment 1.

#### ABSTRACT

You should mention in the abstract that you reconstruct mid-June to mid-Nov (i.e. summer-fall) events, this seems important.

This has been added.

4944-5: See my comment #2 about the term turbidite.

See response to comment 2.

4944-6: See my comment #1 about thickness as intensity proxy.

See response to comment 1.

4944-9: What do you mean with ‘typical of both climatic influences’? You need to explain a bit more here.

This is now better explained:

“typical of both Atlantic (local events) and Mediterranean (meso-scale events) climatic influences”

4944-13to14: You might want to indicate the age range of the MCA and the LIA in years AD.

Age ranges were added.

4944-15: It is not intuitively clear that you refer to high-intensity events with ‘these events’. Please reformulate. Also see my comment #1.

This was changed to: “there is a tendency towards higher frequencies of high-intensity flood events”

4944-18: What do you want to express here? You need to specify more what you mean with ‘uncertainties’, ‘extremes’ and ‘forcing factors’ that you list.

What we mean with ‘uncertainties’ is now explained: “Uncertainties in future evolution of flood intensity”. For ‘extremes’, this refers to the word ‘extremes’ used two sentences above. For ‘forcing factors’, this is now explained: ‘the different climate forcing factors between the two periods’.

#### INTRODUCTION

4945-1: Replace ‘trigger’ with ‘lead to’.

This has been changed.

4945-18: Delete ‘the’ in front of ‘climate variability’.

This has been deleted.

4945-27: ‘: : :: Atlantic in the north and Mediterranean in the south.’

This has been changed.

4945-27: ‘north-western’ part of what? Of the Alps, of the Mediterranean?

This is now indicated: ‘north-western part of the Alps’

4946-3: Please specify. It is not clear what you mean with ‘changes in atmospheric circulation’ and ‘pathways and intensity’. As a reader I would like to see here a short explanation and do not want to extract the necessary information from the references.

This has now been rewritten: ‘...strongly depend on pathways and intensity of storm-tracks’.

4946-10: Rather ‘in this context’ or ‘in this framework’.

This has been changed.

4946-14: Add the country.

This has been added.

#### REGIONAL SETTING

Title 2.1: ‘Hydro-climatic setting and historical flood record’

This has been changed.

4946-17: 'located between the northern and southern French Alps' -> Why not 'central French Alps'?

The French Alps are divided in two parts: the northern French Alps and the southern French Alps. The term 'central French Alps' does not exist.

4946-26: Rather 'to the Queyras massif' instead of 'until'.

This has been changed.

4947-7: 'was' instead of 'have been'.

This has been changed.

4947-16: ': : :', whose hydro-climatic settings are characterized by the south-western and north-western flood pattern, respectively (: : :).'

This has been changed.

4947-22: 'alluvial plain' 4947-22: 'meandering'? This seems rather characteristic for downstream river reaches in settings with a very low slope gradient and not for a mountainous area. Maybe delete the addition about the 'meandering branches' and only use 'alluvial plain'.

This has been changed.

4947-25: 'They enter the lake through only small deltas compared to the Bouchouse inflow area, suggesting limited detrital input.'

This has been changed.

4947-26: What do you mean here with 'glacial deposits'? I expect that this catchment was glaciated in the past, thus I have difficulties to believe that there are no 'glacial deposits' in the forms of sediments (moraines etc.).

There are no evidences of glacial landforms or glacial deposits in the catchment that would suggest the presence of a glacier in the past. In addition, the geological maps published by the BRGM (French Geological Institute; <http://infoterre.brgm.fr/>) do not show any glacial deposits in the catchment area (cf. Fig. 1).

The sentence was modified for clarity:

"There is no evidence that the catchment was glaciated in the past, i.e. no moraine or other glacial deposits."

## METHOD

4948-8: 'was' instead of 'has been'.

This has been changed.

4948-9: Looking at the lake map it rather seems to be the axis between the main inflow (Bouchouse stream) and the outlet.

We changed to: "along a north-south transect in the axis of the two main inlets of the Bouchouse stream"

4948-20: 'Bulk density was used as a proxy for identifying event layers, : : :'. The information about the time ('deposited in a short time') is not necessary in this context, i.e. for detecting the event layers via density, and can be deleted.

This has been deleted.

4949-1to2: What was the concentration of the hydrogen peroxide? What was the temperature of the bath? Did you control after treatment if all organic matter was dissolved (e.g. microscope, organic carbon analysis)?

The sentence was modified for clarity: "...in a bath of diluted (30%) hydrogen peroxyde during 3 days to remove organic matter. After treatment, microscopic observations were performed to control that organic matter was totally dissolved."

4949-3to4: Please specify what you mean with 'transport-deposition dynamics'.

We considered that this term was not useful and we deleted it.

4949-6: 'Grain-size variability' does not reflect the 'maximum discharge volume'. Rather, the grain size is assumed to be proportional to the river discharge. Please reformulate.

The sentence was reworded according to the reviewer 1 comment:

"Grain-size variability is assumed to be related with the stream flow energy of the river entering the lake and, thereby, with the peak discharge reached during the flood event"

4949-12to13: The proposed proportionality of XRF core scanning counts and element concentration is not given for all sediments. Tachikawa et al. (2011) could show this, but it does not necessarily apply to your sediments and the XRF core scanner you used. Without quantitative measurements (e.g. calibration via ICP-MS) I therefore recommend to not interpret element quantities from XRF counts. See also my main comment #3.

See response to comment #3.

4949-23: Rather 'grazing activity' or 'grazing intensity' than 'grazing pressure'.

This has been changed (however, the authors do not understand the difference between these terms).

4949-24: ': : : from the sedimentary abundance of coprophilous: : :'

This has been changed.

4949-27: What is the depth interval of the samples?

This is now indicated in the manuscript: "with an approximate step of 3 cm"

4949-28: Potentially erosive 'event layers' and then on the next line 'turbidites'. This is already a lot of interpretation for a method sections. See also main comment #2.

See the response to the comment #2. The term 'turbidite' was deleted from the manuscript and in this method section, we only speak of 'event layer'.

4950-6: What does 'nb' stand for? I assume number but it is not explained.

'nb' was changed to 'number'.

4950-11: Rather 'For dating the lake sequence: : :'

This has been changed.

4950-13: What do you want to say with 'matching the facies boundaries'? It is the first time that you use these terms here.

The sentence was rewritten for clarity: "The non-regular step aims at matching the facies (i.e. sedimentary background or event layer) boundaries for homogeneous samples."

4950-27: The information about how you modeled the age-depth model should only be given after the paragraph on the paleomagnetic chronological markers.

This has been changed.

4951-3 and following: This is quite a long and detailed explanation on the paleomagnetic chronological markers. Any chance to make this shorter? Or move details into a supplement? What I am missing in this paragraph is actually how you attributed an age to your measurements.

The methods of the palaeomagnetic investigations were shortened in the main manuscript and details were moved into the supplementary material.

## RESULTS

4952 first three paragraphs: See my main comment #2.

See response to comment #2.

4952-21: ': : : over the entire lake basin with a consistent deposition pattern.' Delete 'indeed'. The deposition seems not to be 'regular' in terms of thickness.

'Indeed' was deleted.

4952-24: Please specify what you mean with 'over time'.

'over time' was changed to 'over the studied period'

4953-10: What do you mean with 'well-measured'?

'well-measured' was changed to 'other'.

4953-13: Can you provide evidence or ideas where the Fe is incorporated?

X-ray diffraction analyses were performed in this purpose. However, Fe seems to be associated to many types of clays and the measurements did not appear helpful.

4953-20to23: 'However, since grain-size variability is insignificant, the information that can be won from this proxy in regard flood-intensity reconstruction is minor.' Or similar.

This has been changed as suggested.

4953-24: 'Relative Ca intensities'. Relative to what? See also my main comment #3.

'Relative' indeed appeared inappropriate here and was deleted.

4954-5: You have not yet introduced the abbreviation 'FIT'.

At this stage, the trigger of the deposits is undiscussed. The abbreviations 'MMIL' and 'FIL' are only used as label in figures. This part of text and the figure was reworked in that sense.

4955-26: Abbreviated formulation with parenthesis is not intuitively clear. ‘3 (2) declination (inclination)’

The sentence was reworked for clarity.

4956-6: ‘(without event layers)’

This has been changed.

## DISCUSSION

Title 5.1: ‘Different triggers for event layers’

This has been changed.

4956-18: ‘Ca counts’

This has been changed.

4956-19: Please specify here what you mean with ‘other turbidites’.

This is now specified: ‘the 168 graded layers that not overlain a coarse-grain layer’

4956-24: What would you like to implicate with these angles of delta and littoral slopes?

Do you have numbers for Lake Foréant?

The sentence was changed to address the reviewer’s comment:

‘Slope angles of  $< 10^\circ$  and  $\sim 15^\circ$  for delta and littoral slopes of Lake Foréant, respectively, point to a littoral origin as suggested by many studies showing that slope angles  $> 10^\circ$  are favourable for the generation of mas-movements’.

4956-4-6: These first two sentences do not belong here as they discuss event deposits in general and MMITs, but not flood events.

This has been changed.

4957-9: ‘Ca counts’. See also main comment #3.

See response to comment #3.

4957-17: So what is the effect of oxygen reaching the deeper parts of the basin? I think you should add here the information that Mn-oxides or Mn-hydroxides may precipitate because of this oxygen source.

This is now specified: ‘where it is oxidized and precipitated likely in form of an Mn-oxyhydroxide’

4957-24 and following: This last sentence of the chapter is not clear. E.g. ‘to trigger them’, not clear what is triggered?

This is now specified: ‘flood events are the most probable candidate to trigger the 168 graded layers’

4958-7to8: A lowering of the lake level still seems to be possible. This would lead to slope destabilization.

Lowering of such alpine lake located at high-elevation would imply a negative precipitation/evaporation balance. This is extremely unlikely at this elevation (wet and rather cold climate).

4958-23: ‘Only a few earthquakes’ seems not to be a good expression here, since you wish ‘one single strong earthquake’ in the database in order to be able to attribute a specific age to the deposit.

The sentence was rewritten: ‘For the older period of the third deposit, data of documented earthquakes are sparser in the catalogue, precluding a reliable assignment’

4959-7: You should specify what you mean here with ‘related proxy’ (in parenthesis).

We deleted ‘related proxy’ to avoid confusion.

4959-10 and 4959-8to11: As described under comment #1 I am not convinced that this intensity approximation via flod-layer thickness holds.

See response to comment #1.

4959-20: ‘flood events’ 4959-20 and following: I do not understand what you mean with ‘almost absence’ in regard to documented events of the Bouchouse stream and how that affects your comparison with historical records.

See Table S1, there is only one mention of flood specific to the Bouchouse stream: ‘almost absence’. Hence, an event-to-event comparison between the sedimentary and the historical records cannot be undertaken.

4960-18to19: What exactly should be the difference between a ‘catchment-lake system’ and a ‘river-lake system’? Please specify what you mean and maybe it is clearer when you omit these abbreviations.

Abbreviations were deleted: 'Erosion processes in the Foréant catchment may be affected by modifications in the river system and/or by land-use changes'

4960-22: Rather 'alternating activation'? What 'record' will be disturbed? This does not become clear from the sentence.

This is now specified: 'may disturb the flood record'

4960-28 to 4961-11: Here you address quite well what I mentioned in my comment #1. This alluvial plain is able to store large sediment volumes, which would impact your flood-intensity record. I am particularly concerned because of the very limited grain size variation in the flood deposits. Hence, no information at all about the hydraulic force of the river can be won (i.e. about the river discharge volume).

See response to the comment #1.

4961-21: Here you write 'cells cm<sup>2</sup> yr<sup>-1</sup>', in the method section you wrote 'nb cm<sup>2</sup> yr<sup>-1</sup>'.

This has been changed to be consistent.

4962-8to15: Before you can draw this conclusion you should show that your record relates to the Giguet-Covex record and the former Wilhelm data. Here, it is too early to bring this proposition forward. You should therefore continue here directly with the next paragraph (line 16).

This part was deleted.

4963-3to4: See my main comment #1.

See response to the comment #1.

4963-18to19: Rather ': : : due to moisture advection from the North Atlantic.'

This has been changed as suggested.

4963-19 to 4964-19: You will have to reconsider this discussion on flood intensity. See my main comment #1. Most importantly, if you calculate the ratio of the number of events per century during the LIA (17) and the MCA (10) and you compare it to the ratio of the thickness (LIA: 2.4 mm; MCA: 3.8 mm) you would get very similar values: 1.7 for the number of events and 1.6 for the thickness. Thus, what I want to point out here is that the larger thickness of MCA events could simply be due to the longer storage (thus residence) time of sediment in the catchment. Hence, you would really need the grain size as a flood intensity proxy to make a case here. In addition, you bring forward that the thickness of MCA events (3.8 mm) is 50% larger than the thickness of LIA events (2.4 mm). These '50%' depend on the perspective; one could also argue that LIA events are one third (only) thinner than MCA events.

See response to the comment #1.

4964-23to29: This discussion on possible forcing factors such as solar activity and volcanic eruptions, as well as the possibly different situation during the 20th century due to the increase in greenhouse gas concentrations, comes a bit sudden here. If you wish to keep it you have to elaborate more on the potential influence of the different forcings – even if you say that deeper analysis is necessary.

We appreciate this comment, however, we think that our concise statement should be clear. An elaboration of this in more details would be out of the scope of this paper and require a lot of space. Hence, we did not modify this paragraph.

## CONCLUSIONS

4965-3: Delete 'show'.

This has been deleted.

4965-11to13: Even if there is a consistent depositional pattern in the lake basin, this is unfortunately no proof that the thickness is proportional to flood intensity.

See response to comment #1.

4965-24 to 4966-6: Again, you will have to reconsider your argumentation in regard to flood intensity.

See response to comment #1.

## FIGURES

Figure 2: This figure would profit from a zoom into an interval of about 10 cm length in

order to better demonstrate how geochemical and sedimentological proxies fluctuate between normal sediment and event layers. As it is, it is hard to see how in particular the geochemical proxies vary with the occurrence of event deposits. The unit of the sediment depth is wrong: it should be 'cm' and not 'm'. I assume 'thinner' should be 'finer' (Fe/K column).

The CPD format induced a reduced figure format that was designed to be shown on a whole page (horizontal format). 'Thinner' was changed to 'finer' and 'm' to 'cm'.

Figure 3: The caption could profit from a short explanation why you are plotting this data. (I assume for illustrating the different geochemical characteristics of the different event layers.)

This has been added: 'To illustrate the different geochemical characteristics of the sedimentary background and the graded layers.'

Figure 4: What is 'MP' standing for?

This was indicated in the caption here '(C corresponds to the historic  $^{137}\text{Cs}$  peak of Chernobyl (AD 1986) and MP to the maximum  $^{137}\text{Cs}$  peak of the nuclear fallout (AD 1963)'

Figure 5: Here you need to indicate what the abbreviations D-1 etc. and I-1 etc. stand for. stands for. This is also necessary because the abbreviation appear in the following figures.

This has been added: 'The well-correlated declination and inclination features are labelled D-x and I-x, respectively.'

Figure 7: Please indicate in the caption that the question mark refers to a possible gap (am I correct?) in the historical data.

This has been added as suggested.

# 1 Frequency and intensity of palaeofloods at the interface of 2 Atlantic and Mediterranean climate domains

3  
4 **B. Wilhelm<sup>1,2</sup>, H. Vogel<sup>2</sup>, C. Crouzet<sup>3,4</sup>, D. Etienne<sup>5</sup>, F.S. Anselmetti<sup>2</sup>**

5  
6 [1]{Univ. Grenoble Alpes, LTHE, F-38000 Grenoble, France}

7 [2]{Institute of Geological Sciences and Oeschger Centre for Climate Change Research,  
8 Univ. of Bern, CH-3012 Bern, Switzerland}

9 [3]{Univ. Savoie Mont Blanc, ISTerre, F-73376 Le Bourget-du-Lac, France}

10 [4]{CNRS, ISTerre, F-73376 Le Bourget-du-Lac, France}

11 [5]{UMR INRA 42 CARRTEL, Univ. Savoie Mont Blanc, F-73376 Le Bourget du Lac,  
12 France}

13 Correspondence to: B. Wilhelm (bruno.wilhelm@ujf-grenoble.fr)

## 14 15 **Abstract**

16 The long-term response of the flood activity to both Atlantic and Mediterranean climatic  
17 influences was explored by studying a lake sequence (Lake Foréant) of the Western European  
18 Alps. High-resolution sedimentological and geochemical analysis revealed 171 **event layers**,  
19 168 of which result from past flood events over the last millennium. The **layer** thickness was  
20 used as a proxy of intensity of past floods. Because the Foréant palaeoflood record is in  
21 agreement with the documented variability of historical floods resulting from local and  
22 mesoscale, **summer-to-autumn** convective events, it is assumed to highlight changes in flood  
23 frequency and intensity related to such events typical of both **Atlantic (local events) and**  
24 **Mediterranean (meso-scale events)** climatic influences. Comparing the Foréant record with  
25 other Atlantic-influenced and Mediterranean-influenced regional flood records highlights a  
26 common feature in all flood patterns that is a higher flood frequency during the cold period of  
27 the Little Ice Age (LIA, **AD 1300-1900**). In contrast, high-intensity flood events are apparent  
28 during both, the cold LIA and the warm Medieval Climate Anomaly (MCA, **AD 950-1250**).  
29 However, there is a tendency towards higher frequencies of **high-intensity flood** events during  
30 the warm MCA. The MCA extremes could mean that under the global warming scenario, we  
31 might see an increase in intensity (not in frequency). However, the flood frequency and  
32 intensity in course of 20<sup>th</sup> century warming trend did not change significantly. Uncertainties **in**

33 **future evolution of flood intensity** lie in the interpretation of the lack of 20<sup>th</sup> century extremes  
34 (transition or stable?) and the different climate forcing factors **between the two periods**  
35 (greenhouse gases vs. solar/volcanic eruptions).

36

37 **Key-words:** palaeoflood record, flood frequency, flood intensity, Atlantic influence,  
38 Mediterranean influence, last millennium

39

## 40 **1. Introduction**

41 Heavy rainfall events trigger mountain-river floods, one of the most significant natural  
42 hazards, causing widespread loss of life, damage to infrastructure and economic deprivation  
43 (e.g. **Kundzewicz et al., 2014**). This is especially the case for the Alpine area in Europe,  
44 where tourism and recent demographic development with an increasing population raise the  
45 vulnerability of infrastructure to natural hazards (e.g. Beniston and Stephenson 2004).  
46 Moreover, the current global warming is expected to **lead to** an intensification of the  
47 hydrological cycle and a modification of flood hazard (IPCC et al., 2013). Hence, a robust  
48 assessment of the future evolution of the flood hazard over the Alps becomes a crucial issue.

49 A main limitation for robust flood-hazard projections is the scarce knowledge on the  
50 underlying natural climate dynamics that lead to these extreme events (IPCC, 2013). Indeed,  
51 the stochastic nature and the rare occurrence of extreme events make the identification of  
52 trends based on instrumental data alone difficult (e.g. Lionello et al., 2012). One way of  
53 overcoming this issue is to extend flood series beyond observational data and compare these  
54 datasets with independent climatic and environmental forcing. In this purpose, many types of  
55 sedimentary archives have been studied (e.g. Luterbacher et al., 2012 and references therein).  
56 Among them lake sediments are being increasingly studied because they allow to reconstruct  
57 flood records long enough to identify the natural variability at different time scales (e.g.  
58 Noren et al., 2002; Osleger et al., 2009; Wilhelm et al., 2012a; Czymzik et al., 2013; Glur et  
59 al., 2013; Corella et al., 2014).

60 In the western Alps, many lake-sediment sequences have been studied to better assess the  
61 response of the flood activity to climate variability. These studies revealed higher flood  
62 frequency of mountain streams in many regions during multi-centennial cold phases such as  
63 the Little Ice Age (Giguet-Covex et al., 2012; Wilhelm et al., 2012a; 2013; Glur et al., 2013;  
64 Wirth et al., 2013b; Amann et al., 2015). However, regarding flood intensity/magnitude,

65 opposite patterns appear with the occurrence of the most extreme events during warmer  
66 periods in the north (Giguet-Covex et al., 2012; Wilhelm et al., 2012b; 2013), while they  
67 occurred during colder periods in the south (Wilhelm et al., 2012a; 2015). These north-south  
68 opposite flood patterns were explained by flood-triggering meteorological processes specific  
69 to distinct climatic influences: **Atlantic in the north versus Mediterranean in the south**. In the  
70 north-western part **of the Alps**, floods at high altitude are mainly triggered by local convective  
71 events (i.e. thunderstorms) and seem to mainly depend on the temperature that would  
72 strengthen vertical processes (e.g. Wilhelm et al., 2012b; 2013). In contrast, floods in the  
73 south are mostly triggered by mesoscale events and may strongly **depend on pathways and**  
74 **intensity of storm-tracks** (e.g. Trigo and Davis, 2000; Boroneant et al., 2006; Boudevillain et  
75 al., 2009). By analogy with these results over past warm periods, the mountain-flood hazard  
76 might be expected to increase in the north-western Alps, mainly because of an enhanced flood  
77 magnitude associated to stronger convective processes. Hence, better assessing the spatial  
78 extent of the Atlantic-influenced flood pattern at high-altitude appears a crucial issue to  
79 appropriately establish hazard mitigation plans and prevent high socio-economic damages.

80 In this context, the present study was designed to reconstruct the flood pattern at an  
81 intermediate situation between the north-western and south-western Alps, i.e. at the climate  
82 boundary between Atlantic and Mediterranean influences. This is undertaken by  
83 reconstructing a millennium-long flood chronicle from the sediment sequence of the high-  
84 altitude Lake Foréant located in the Queyras Massif **(France)**.

85

## 86 **2. Regional setting**

87

### 88 **2.1. Hydro-climatic setting and historical flood record**

89 The Queyras massif is located in between the northern and southern French Alps where the  
90 climate is influenced by the Atlantic Ocean and the Mediterranean Sea (Fig. 1). As a result,  
91 the Queyras mountain range corresponds to a transition zone of Alpine precipitation patterns  
92 in the meteorological reanalyses (Durant et al., 2009; Plaut et al., 2009) and in the simulations  
93 (Frei et al., 2006; Rajczak et al., 2013). In the Queyras, heavy precipitation events are related  
94 to either local convective phenomena (i.e. summer thunderstorms) or mesoscale convective  
95 systems. The mesoscale systems called “Lombarde-Type” or “East Return” events occur  
96 mainly from late spring to fall and result from Mediterranean humid air masses flowing

97 northward into the Po Plain and then westward to the Queyras Massif (e.g. Gottardi et al.,  
98 2010; Parajka et al., 2010). The humid air masses are then vigorously uplifted with the steep  
99 topography of the Queyras massif, causing an abrupt cooling of the air masses and intense  
100 precipitations. Such mesoscale precipitation events, typical of the Mediterranean climate (e.g.  
101 Buzzi and Foschini, 2000; Lionello et al., 2012), affect extensive areas and may lead to  
102 catastrophic floods at a regional scale as shown in June 1957 or October 2000 over the  
103 Queyras massif (Arnaud-Fassetta and Fort, 2004). Other numerous past flood events were  
104 documented from studies of local historical records. These data have been compiled in a  
105 database managed by the ONF-RTM (<http://rtm-onf.ifn.fr/>). They show that the village of  
106 Ristolas (located 8 km downstream from Lake Foréant, Fig. 1C) has been affected at least 34  
107 times over the last 250 years by floods of the Guil River and its five main tributaries (see  
108 Supplementary Material).

109

## 110 **2.2. Lake Foréant and its tributaries**

111 Lake Foréant (2620 m a.s.l., 44°42'20"N, 6°59'00"E) is located in a cirque of 3 km<sup>2</sup> in the  
112 upper part of the Queyras Massif, adjacent to the Italian border (Fig. 1). It is located  
113 approximately 60 km north from Lake Allos and 100 km south-west from Lakes Blanc,  
114 whose hydro-climatic settings are characterized by the south-western and north-western flood  
115 pattern, respectively (Wilhelm et al., 2012a,b; Fig. 1B). The catchment rises up to 3210 m.  
116 a.s.l. and is made up of three lithologies from the Queyras schistes-lustrés nappe (e.g.  
117 Schwartz et al., 2009); (i) marble in the eastern part, (ii) calc-schist in the western part and  
118 (iii) a narrow band of arkose in between (Fig. 1D). The main stream of the catchment, the  
119 Torrent de Bouchouse, drains mainly the central band of arkose. Before entering the lake, this  
120 stream has built an alluvial plain (Fig. 1E). This suggests that the Bouchouse stream is a  
121 major source of sediment entering the lake. In addition, two minor and non-permanent  
122 streams drain the western part of the catchment. In contrast, they enter the lake through only  
123 small deltas compared to the Bouchouse inflow area, suggesting limited detrital inputs. There  
124 is no evidence that the catchment was glaciated in the past, i.e. no moraine or other glacial  
125 deposits occur. Thereby, detrital inputs only result from the erosion and transport of these  
126 lithologies. Detrital inputs from these streams are limited to summer and fall because the  
127 catchment is covered by snow and the lake is frozen from mid-November to the beginning of  
128 June. The Bouchouse stream flows downstream into the Guil River and reaches  
129 approximately 8 km further the village of Ristolas (Fig. 1C).

130

### 131 **3. Method**

132

#### 133 **3.1. Lake coring**

134 In summer 2013, a bathymetric survey was carried out on Lake Foréant and revealed a well-  
135 developed flat basin in the centre of the lake with a maximum water depth of 23.5 m (Fig.  
136 1E). An UWITEC gravity corer **was** used to retrieve four cores along a north-south transect in  
137 the axis of the two main inlets **of the Bouchouse stream**. Cores FOR13P3 and FOR13P4  
138 correspond to the proximal locations of the two different branches of the Bouchouse stream  
139 and aim at investigating their respective sediment inputs during floods. Cores FOR13P2 and  
140 FOR13P1 correspond to the depocenter and to the most distal position, i.e. the opposite slope  
141 to the Bouchouse inflows, respectively.

142

#### 143 **3.2. Core description and logging**

144 Cores were split lengthwise and the visual macroscopic features of each core were examined  
145 to identify the different sedimentary lithofacies. The stratigraphic correlation between the  
146 cores was then carried out based on these defined lithofacies. **The stratigraphic correlation**  
147 **allows identifying the depositional pattern of the event layers within the lake basin.**  
148 **Depositional patterns of event layers may help to decipher their trigger, i.e. mass-movements**  
149 **vs. flood events (e.g. Sturm and Matter, 1978; Wilhelm et al., 2012b; Van Daele et al., 2015).**

150 High-resolution color line scans and gamma-ray attenuation bulk density measurements were  
151 carried out on a Geotek™ multisensor core-logger (Institute of Geological Sciences,  
152 University of Bern). Bulk density was used as a proxy of event layers, e.g. flood **layers**,  
153 characterized by higher density due to the high amount of detrital material (e.g. Støren et al.,  
154 2010; Gilli et al., 2012; Wilhelm et al., 2012b).

155 Geochemical analysis and X-ray imaging were carried out using an Itrax™ (Cox Analytical  
156 Systems) X-ray fluorescence (XRF) core scanner (Institute of Geological Sciences, University  
157 of Bern), equipped with a Molybdenum tube (50 keV, 30 mA) with a 10-s count-time using  
158 sampling steps of 1 mm (XRF) and 0.2 mm (X-ray imaging). The areas of the element peaks  
159 obtained are proportional to the concentrations of each element (Tachikawa et al., 2011).  
160 Geochemical data were applied to identify **event layers** at high resolution through their higher

161 content in detrital material (e.g. Arnaud et al., 2012; Wilhelm et al., 2012b; Czymzik et al.,  
162 2013; Swierczynski et al., 2013) and/or as high-resolution grain-size proxies (e.g. Cuven et  
163 al., 2010; Wilhelm et al., 2012a; 2013). Geochemical analyses were carried out on core  
164 FOR13P2. X-ray images highlighting the variability of the sediment density have been  
165 acquired for the four cores.

166 Grain size analyses on core FOR13P2 were performed using a Malvern Mastersizer 2000  
167 (Institute of Geography, University of Bern) on sub-samples collected at a 5-mm continuous  
168 interval. Before grain-size analysis, the samples were treated in a bath of diluted (30%)  
169 hydrogen peroxyde during 3 days to remove organic matter. After treatment, microscopic  
170 observations were performed to control that organic matter was totally dissolved. These grain-  
171 size analyses of the detrital material were performed to characterize event layers and, when  
172 event layers are induced by floods, to establish a proxy of flood intensity. Grain-size  
173 variability is assumed to be related with the stream flow energy of the river entering the lake  
174 and, thereby, with the peak discharge reached during the flood event (Campbell, 1998;  
175 Lapointe et al., 2012; Wilhelm et al., 2015). The flood intensity may also be reconstructed  
176 based on the amount of sediment transported and deposited during floods (e.g. Schiefer et al.,  
177 2011; Jenny et al., 2014; Wilhelm et al., 2015). This approach appeared particularly relevant  
178 in case of an insignificant variability of the flood-sediment grain size (e.g. Jenny et al., 2014;  
179 Wilhelm et al., 2015). When the depositional pattern of the flood layers within the lake basin  
180 (assessed through the stratigraphic correlation) shows a high variability, many cores are  
181 required for a reliable assessment of the flood-sediment volumes (e.g. Page et al., 1994;  
182 Schiefer et al., 2011; Jenny et al., 2014). However, when the depositional pattern of the flood  
183 layers is stable over time, the layer thickness in one core may be sufficient (e.g. Wilhelm et  
184 al., 2012b; 2015). As a result, grain size and sediment volume of the event layers were both  
185 explored as two distinct proxies of flood intensity.

186

### 187 3.3. Coprophilous fungal spores analysis

188 Erosion processes in high-altitude catchments may be modified by grazing activity and,  
189 thereby, the climatic signal in flood reconstructions may be altered (e.g. Giguet-Covex et al.,  
190 2012). The variability of grazing intensity in a catchment area can be reconstructed from the  
191 sedimentary abundance of coprophilous fungal ascospores, i.e. *Sporormiella* (HdV-113) (e.g.  
192 Davis and Schafer, 2006; Etienne et al., 2013). To test the potential impact of grazing

193 intensity on the reconstructed flood activity, *Sporormiella* abundance was determined in  
194 subsamples collected all along the core FOR13P3 with an approximate step of 3 cm. This core  
195 was chosen because it was the sequence with the thinnest potentially-erosive event layers.  
196 During the sampling, event layers were avoided because they may correspond to layers  
197 induced by flood or mass-movement events that may have transported unusual quantities of  
198 *Sporormiella* ascospores, or induced the remobilization of older sediments. Subsamples were  
199 chemically prepared according to the procedure of Fægri and Iversen (1989). *Lycopodium*  
200 *clavatum* tablets were added in each subsample (Stockmarr, 1971) to express the results in  
201 concentrations (number.cm<sup>-3</sup>) and accumulation rates (number.cm<sup>2</sup>.yr<sup>-1</sup>). Coprophilous fungal  
202 ascospores were identified based on several catalogues (Van Geel and Aptroot, 2006; Van  
203 Geel et al., 2003) and counted following the procedure established by Etienne and Jouffroy-  
204 Bapicot (2014).

205

#### 206 3.4. Dating methods

207 For dating the lake sequence over the last century, short-lived radionuclides (<sup>210</sup>Pb, <sup>137</sup>Cs)  
208 were measured by gamma spectrometry at the EAWAG (Zürich, Switzerland). The core  
209 FOR13P4 was sampled following a non-regular step of 1±0.2 cm. The non-regular step aims  
210 at matching the facies (i.e. sedimentary background or event layer) boundaries for  
211 homogeneous samples. The <sup>137</sup>Cs measurements allowed two main chronostratigraphic  
212 markers to be located: the fallout of <sup>137</sup>Cs from atmospheric nuclear weapon tests culminating  
213 in AD 1963 and the fallout of <sup>137</sup>Cs from the Chernobyl accident in AD 1986 (Appleby,  
214 1991). The decrease in excess <sup>210</sup>Pb and the Constant Flux/Constant Sedimentation (CFCS)  
215 allowed a mean sedimentation rate to be calculated (Goldberg, 1963). The standard error of  
216 the linear regression of the CFCS model was used to estimate the uncertainty of the  
217 sedimentation rate obtained by this method. The <sup>137</sup>Cs chronostratigraphic markers are then  
218 used to control the validity of the <sup>210</sup>Pb-based sedimentation rate.

219 To date the sequence beyond the last century, small-size vegetal macro-remains were sampled  
220 in core FOR13P4. Terrestrial plant remains were isolated at the Institute of Plant Sciences  
221 (University of Bern) and sent for AMS <sup>14</sup>C analysis to the AMS LARA Laboratory  
222 (University of Bern). <sup>14</sup>C ages were calibrated using the Intcal13 calibration curve (Reimer et  
223 al., 2013; Table 1). In addition, palaeomagnetic chronostratigraphic markers were also used.  
224 These markers can be obtained by comparing the characteristic declination and inclination of

225 remanent magnetization (ChRM) versus depth to global geomagnetic models or to known  
226 secular variations of the geomagnetic field (e.g. Barletta et al., 2010; Wilhelm et al., 2012a).  
227 Palaeomagnetic investigations were performed at the CEREGE laboratory (University Aix-  
228 Marseille) and are detailed in supplementary material.

229 Using the R-code package “clam” (Blaauw, 2010), an age-depth model was generated from  
230 the  $^{210}\text{Pb}$  ages, the  $^{14}\text{C}$  ages and the palaeomagnetic chronological markers.

231

## 232 4. Results

233

### 234 4.1. Sedimentology

235 The sediment consists of a homogeneous, brown mud mainly composed of silty detrital  
236 material and aquatic organic remains (small fragments of plants and anamorphous organic  
237 matter), representing the background hemi-pelagic sedimentation. These fine grained deposits  
238 are interrupted by 171 rather coarser-grained layers, which are interpreted to represent short-  
239 term depositional events, i.e. event layers (Fig. 2).

240 The 171 event layers correspond to graded layers, characterized by their higher density, a  
241 slight fining-upward trend and a thin, whitish fine-grained capping layer (Fig. 2). There is no  
242 evidence of an erosive base. According to the stratigraphic correlation, almost all these graded  
243 layers (168 out of 171) extend over the entire lake basin with a regular deposition pattern. The  
244 thickness of these 168 graded layers is systematically larger in cores FOR13P2 and FOR13P4,  
245 and decreases respectively in cores FOR13P1 and FOR13P3. This suggests that the southern  
246 branch of the Bouchouse stream is the main sediment input over the studied period (Fig. 1).  
247 The grain-size of these graded layers is dominated by silt-sized grains with only small  
248 amounts of clay / fine silt present in the whitish capping layer and to coarse silt in their basal  
249 part (Fig. 2). The origin of these 168 is discussed in section 5.1. The three other graded layers  
250 show a higher variability in thickness, grain size and depositional pattern. Above all, they  
251 overlie three cm-thick coarse-grained layers, present at 75 cm in core FOR13P2 and at 9 and  
252 42 cm in core FOR13P4 (Fig. 2). The coarse-grained layers consist of pebble gravels and  
253 aquatic plant remains embedded in a silty matrix. The high porosity in the sediment due to the  
254 presence of gravels generates a partial loss of XRF signal, preventing a reliable geochemical  
255 characterization. X-ray images show chaotic sedimentary structures. The stratigraphic  
256 correlation revealed that two centimetres of sediment are missing below the thickest coarse-

257 grained layer in core FOR13P4, suggesting an erosive base for this layer. The stratigraphic  
258 succession of a coarse-grained layer overlain by a graded layer (labelled MMIL in Fig. 2 and  
259 3) suggests that the two layers were induced by a single event. Their origin is discussed in  
260 section 5.1.

261

## 262 4.2. Geochemistry

263 Among the core scanner output parameters, the scattered incoherent (Compton) radiation of  
264 the X-ray tube ( $Mo_{inc}$ ) may vary with the sediment density (Croudace et al., 2006) and,  
265 thereby, offer a high-resolution proxy for sediment density.  $Mo_{inc}$  values were averaged at a  
266 5-mm resolution to be compared to the density obtained at a 5-mm resolution with the  
267 gamma-ray attenuation method. A positive and significant correlation ( $r=0.85$ ,  $p<10^{-4}$ )  
268 between the two density parameters was found and allowed using  $Mo_{inc}$  as a proxy of  
269 sediment density for identifying millimetre-scale event layers (Fig. 3).

270 The variability of other elements within the event layers was then investigated to assess i) a  
271 high-resolution grain-size proxy and ii) distinct sediment sources of the event layers between  
272 the littoral (i.e. mass-movement origin) and the catchment area (i.e. flood origin). The  
273 variability of potassium (K) intensities vs. sediment depth (Fig. 3) shows increased K  
274 intensities in the capping layers of the event layers, suggesting K enrichment in the finest  
275 sediment fraction. Variability in silicon (Si) intensities is correlated to K intensities ( $r=0.77$ ,  
276  $p<10^{-4}$ ). Variations in iron (Fe) intensities show an opposite pattern with Fe enrichments in  
277 the basal and coarser part of the graded beds. Interestingly, Fe is the only element which  
278 elevated in event layers. These results suggest that the Fe/K ratio may be used as a millimetre-  
279 scale proxy for relative grain-size distribution and hence for detecting millimetre-scale event  
280 layers. However, since grain-size variability is insignificant, the information that can be won  
281 from this proxy in regard to flood-intensity reconstruction is minor.

282 Ca intensities are most of the time very low ( $< 900$  counts), except for several sharp peaks and  
283 two well-marked excursions ( $> 1200$  counts) at 30 and 75 cm in core FOR13P2 (Fig. 3).  
284 These two well-marked excursions correspond to the two thickest graded layers (labelled  
285 MMIL2 and 3; Fig. 2). In addition, manganese (Mn) intensities also vary within a low value  
286 range ( $< 10^4$  counts) interrupted by sharp, well-marked peaks (up to  $4 \cdot 10^4$  counts). All those  
287 Mn peaks are located at the base of the 168 graded layers (those that not overlain a coarse-  
288 grain layers). However not every base of graded layers corresponds to a Mn peak. To better

289 assess the relationships between those elements, the Ca intensities were plotted against Fe, K  
290 and Mn intensities (Fig. 3). These plots clearly highlight two groups of deposits. The  
291 background sediments and the 168 graded layers (those labelled FIL in Fig. 3) are  
292 characterized by i) low Ca intensities and ii) a high variability in Mn intensities. The three  
293 graded layers labelled MMIL in figure 2 show a distinct geochemical pattern with (i) high Ca  
294 intensities regardless of Fe and K intensities and (ii) very low Mn intensities.

295

### 296 4.3. Chronology

297 The down-core  $^{210}\text{Pb}$  excess profile for core FOR13P2 shows a continuous decrease to low  
298 values ( $\sim 50 \text{ Bq.Kg}^{-1}$ ), punctuated by sharp excursions to low values for three layers (2-3.5  
299 cm, 7.5-10.5 cm and 15-17 cm) corresponding to graded layers (Fig. 4A). In line with Arnaud  
300 et al. (2002), these values were excluded to build a corrected sedimentary record without  
301 event layers (Fig. 4B). The CFCS model (Goldberg, 1963), applied on the event-free  $^{210}\text{Pb}$   
302 excess profile, provides a mean sedimentation rate of  $1.3 \pm 0.1 \text{ mm.yr}^{-1}$  (without the event  
303 layers). Ages derived from the CFCS model were transposed to the original sediment  
304 sequence to provide a continuous age-depth relationship (Fig. 4C). The event-free  $^{137}\text{Cs}$   
305 profile indicated two peaks at 3.5 cm and 5.5 cm (Fig. 4B), interpreted as the result of the  
306 Chernobyl accident in AD 1986 and the maximum fallout of the nuclear weapon tests in AD  
307 1963. These independent chronological markers are in good agreement with the  $^{210}\text{Pb}$  excess  
308 ages, supporting the age-depth model over the last century (Fig. 4C).

309 In order to evaluate the reliability and efficiency of the palaeomagnetic results several points  
310 need to be verified: i) the preservation of the sedimentary magnetic fabric, ii) the stability of  
311 magnetic mineralogy, and iii) the stability of the magnetic components. Results of Anisotropy  
312 of Magnetic Susceptibility for core FOR13P4 show a well preserved sedimentary fabric, i.e.  
313 Kmin inclination close to the vertical, except in the thickest event layers (labelled MMIL2  
314 and MMIL3, Fig. 2) where the Kmin inclination is clearly deviated (Fig. S1). For the 3 cores,  
315 the mean destructive field of ARM and IRM is very similar (between 20 and 30 mT)  
316 indicating a magnetic mineralogy mainly composed of low coercivity phase. The S-ratio  
317 (Bloemendal et al., 1992) is always between 0,86 and 0,95 indicating lower coercivity and a  
318 ferrimagnetic mineralogy. This suggests a good stability of the magnetic mineralogy, except  
319 in event layers where other parameters such as the relative palaeointensity (calculated as  
320 NRM intensity divided by ARM intensity) are clearly different, highlighting a different

321 magnetic mineralogy. PCA have then been performed using puffin plot software (Lurcock  
322 and Wilson, 2012) to calculate the ChRM. A careful examination of demagnetization  
323 diagrams shows a unidirectional behaviour (Fig. S2). The Mean Angular Deviation (MAD) is  
324 usually lower than 6 revealing a good stability of the magnetization direction. In most cases,  
325 the calculated component is not straight to the origin. This is particularly the case in the event  
326 layers. This implies the occurrence of a high coercivity component of unknown origin. All  
327 cores show quite large variations of the declination and inclination *vs.* depth. Because of the  
328 deviation of the Kmin and changes in magnetic mineralogy, measurements from the thickest  
329 event layers (i.e. MMIT2 and MMIT3) have been removed to build event-free declination and  
330 inclination signals (Fig. 5A). Based on the stratigraphic correlation, the event-free  
331 palaeomagnetic profiles obtained for each core were all corrected to a reference depth, i.e. the  
332 event-free depth of core FOR13P2 (Fig. 5B). Finally, all magnetic profiles were averaged to  
333 obtain unique curves of declination *vs.* depth and inclination *vs.* depth (Fig. 5C), smoothing  
334 small artefacts and making it easier for comparison to the reference curve (ARCH3.4k model;  
335 Donadini et al., 2009; Korte et al., 2009). From the variations of the reference curve over the  
336 last millennium, magnetic declination minima and maxima can be identified at AD 1810  $\pm$ 20,  
337 1540  $\pm$ 70 and 1365  $\pm$ 25 (D-1 to D-3, respectively). For the inclination, two tie points at AD  
338 1700  $\pm$ 30 and 1330  $\pm$ 40 can be used (I-1 and I-2, Fig. 5D). Furthermore **the ChRM**  
339 **declination profile presents 3 declination features and the ChRM inclination profile presents 2**  
340 **inclination features over this period,** allowing the correlation proposed (Fig. 5). These well-  
341 correlated declination and inclination features can thus be used as additional chronological  
342 markers.

343 The  $^{210}\text{Pb}$  and the  $^{14}\text{C}$  ages (Fig. 4 and Table 1) were then combined with the palaeomagnetic  
344 chronomarkers (Fig. 5) to construct an age-depth model covering the whole sequence (Fig. 6).  
345 As noted above, the age-depth model was calculated on an event-free depth using a smooth  
346 spline with the “clam” R-code package (Blaauw, 2010). This revealed that the sequence FOR  
347 covers the last millennium with a mean sedimentation rate of 1 mm.yr<sup>-1</sup> (without event  
348 layers).

349

## 350 **5. Discussion**

351

## 352 **5.1. Different triggers for event layers**

353

### 354 **5.1.1. Mass movements**

355 The unusual presence of gravel and aquatic plant remains, in combination with the chaotic  
356 sedimentary structures and the localized deposition areas, suggest that the coarse-grained  
357 layers result of a mass movement originating from sediment-charged slopes (e.g. Sauerbrey et  
358 al., 2013). The three graded layers overlying the coarse-grained layers are then resulting from  
359 the sediment that is transported in suspension during sliding of subaquatic slope sediments  
360 and then deposited over the coarse-grained layers and further into the lake basin (e.g.  
361 Girardclos et al., 2007; Moernaut et al., 2014). As a result, each stratigraphic succession of a  
362 graded and a coarse-grained layer is interpreted as a mass-movement-induced layer (MMIL).  
363 These MMILs are well characterized by higher Ca intensities that suggest a distinctly  
364 different sediment source when compared to the sedimentary background and to the 168  
365 graded layers that not overlain a coarse-grain layer. The coarse-grained layer of MMIL3 is  
366 only present in core FOR13P3, suggesting a littoral origin of the mass movement (Fig. 2). The  
367 two coarse-grained layers of MMIL1 and MMIL2 are located in core FOR13P4 (Fig. 2).  
368 These layers may thus originate either from the delta or from the littoral slopes. Slope angles  
369 of  $< 10^\circ$  and  $\sim 15^\circ$  for delta and littoral slopes of Lake Foréant, respectively, point to a littoral  
370 origin as suggested by many studies showing that slope angles  $> 10^\circ$  are favourable for the  
371 generation of mass-movements (e.g. Moernaut et al., 2007; Strasser et al., 2011; Van Daele et  
372 al., 2013). In addition, higher Ca intensities are often an indicator of littoral sediments as a  
373 result of increased fluxes of endogenic calcite when compared to the open-water endogenic  
374 production.

375

### 376 **5.1.2. Flood events**

377 The 168 graded layers may be induced by either mass movements or flood events (e.g. Sturm  
378 and Matter, 1978). Their extents over the whole basin with a relatively homogeneous  
379 deposition pattern, their frequent occurrence and a different geochemical pattern suggest a  
380 distinct origin from that of the MMIL graded layers. The low Ca intensities suggest a minor  
381 sediment contribution of the marble and calc-schists in favour of a major contribution of the  
382 arkose band, which is the lithology drained by the main inflow (Fig. 1). The 168 graded layers  
383 are also characterized by sharp peaks of Mn only located at their bases. This location suggests

384 that the punctual enrichment in Mn is related to the occurrence of these event layers. Mn is a  
385 redox sensitive element and more soluble under reducing conditions (e.g. Davison, 1993;  
386 Torres et al., 2014). The punctual presence of detectable Mn at the base of the **graded layers**  
387 suggests that hyperpycnal turbidity currents carry oxygen to the deeper parts of the basin.  
388 Dissolved oxygen is probably also trapped in pore waters of the individual **graded layers**.  
389 Based on these considerations we suggest that dissolved and reduced Mn is, in part due to the  
390 rapid increase in loading from the **graded layers**, migrating from pore waters of the buried  
391 sediments into oxygenated **graded layers** where it is oxidized and precipitated likely in form  
392 of an **Mn**-oxyhydroxide (e.g. Davison, 1993; Deflandre et al., 2002). The fast sediment  
393 deposition during the event-layer formation and the low reactive organic matter  
394 concentrations would then prevent reductive dissolution of the Mn-oxyhydroxide precipitates  
395 (e.g. Torres et al., 2014). According to these **layer** characteristics, flood events are the most  
396 probable candidate to trigger the **168 graded layers** because i) these events may be frequent  
397 (e.g. Czymzik et al., 2013), ii) these events may bring both high oxygen and detrital inputs in  
398 a short time (e.g. Deflandre et al., 2002), and iii) the nature of the sediment correspond the  
399 most to the main lithology drained by the inflow. Hence, the 168 **graded layers** likely  
400 correspond to flood-induced **layers (FIL)**.

401

### 402 **5.1.3. Chronological controls**

403 **MMILs** can be triggered by spontaneous failures due to overloading/oversteepening of  
404 sediments-charged slopes, snow avalanches, rockfalls, earthquakes or fluctuations in lake  
405 levels (e.g. Monecke et al., 2004; Girardclos et al., 2007; Moernaut et al., 2014). In case of  
406 Lake Foréant, changes in lake level can be excluded because water levels of Lake Foréant are  
407 well controlled by bedrock outlets. In addition, there is no geomorphological evidence of  
408 major rockfalls in the catchment area. Regarding earthquakes, many events occurred in the  
409 region and affected the population and infrastructure. Historical earthquakes are well  
410 documented thanks to the database SisFrance (<http://www.sisfrance.net>, Lambert and Levret-  
411 Albaret, 1996; Scotti et al., 2004). An earthquake trigger for the **MMILs** can then be  
412 investigated by comparing ages of the **MMILs** to the dates of the closest and/or strongest  
413 historical earthquakes (e.g. Avşar et al., 2014; Howarth et al., 2014). The three **MMILs** are  
414 respectively dated to AD 1963 ( $\pm 6$ ), AD 1814 (+50/-39) and AD 1456 (+19/-56) (Fig. 6). The  
415 age of the most recent deposit is consistent with the Saint-Paul-sur-Ubaye earthquake (AD  
416 1959), characterized by an epicentre at ca. 20 km from the lake where the MSK intensity

417 reached VII-VIII. The age of the second deposit is consistent with the Piemont (Torre Pellice)  
418 earthquake (AD 1808), characterized by an epicentre at ca. 20 km from the lake and a MSK  
419 intensity of VIII (Fig. 6). For the older period of the third deposit, data of documented  
420 earthquakes are sparser in the catalogue, precluding a reliable assignment. The earthquakes of  
421 Saint-Paul-sur-Ubaye and Piemont are both the closest and strongest historically-known  
422 earthquakes around the lake, suggesting that they are the most probable trigger of the  
423 temporarily corresponding subaquatic landslides. Overall, there is a good agreement between  
424 major historical events and the calculated ages of the MMILs supporting their sedimentologic  
425 interpretation and the chronology over the last centuries.

426

## 427 5.2. Palaeoflood record

428 A flood chronicle of the Bouchouse stream was built by dating the 168 FILs over the last  
429 millennium. Changes in flood frequency are highlighted through a running sum of flood  
430 occurrences with an 11-year (Fig. 7) or 31-year window (Fig. 8). The absence of significant  
431 grain-size variability precludes the use of grain size to assess changes in flood intensity (e.g.  
432 Giguet-Covex et al., 2012; Lapointe et al. 2012; Wilhelm et al., 2013, 2015). The relatively  
433 homogeneous grain size of the FILs makes the sediment accumulation per event a more  
434 suitable proxy of flood intensity (e.g. Jenny et al., 2014). In addition, the relatively  
435 homogeneous flood-sediment deposition pattern within the lake basin makes it possible to use  
436 the FIL thickness as a proxy of the flood-sediment accumulation as shown by previous  
437 calibration in Alpine environments (Wilhelm et al., 2012b; Jenny et al., 2014; Wilhelm et al.,  
438 2015). Hence, the FIL thickness is here assumed to represent the flood intensity, under the  
439 condition that erosion processes and availability of erodible materials in the catchment did not  
440 change significantly over time.

441

### 442 5.2.1. Proxy validation

443 To control the reliability of our reconstruction, the Foréant palaeoflood record is compared to  
444 the historical floods at Ristolas located around 8 km downstream the lake (Fig. 1C and  
445 Supplementary Material). The almost absence of documented flood event for the Bouchouse  
446 stream (outlet of Lake Foréant) precludes an event-to-event comparison as undertaken with  
447 the Lake Allos record (Wilhelm et al., 2015). Hence, the 21 flood events having affected the  
448 village of Ristolas and occurring during the ice-free season of the lake (mid-June to mid-

449 November) have been considered to reconstruct a historical flood record (Fig. 7). This  
450 includes 6 floods considered as ‘local’ because they only affected the village of Ristolas  
451 (catchment area of ca. 80 km<sup>2</sup>) and 15 floods considered as ‘sub-regional’ because they also  
452 affected other villages downstream (Abriès, Aiguilles, Chateau-Vieille-Ville, catchment area  
453 of ~320 km<sup>2</sup>). Through comparison of the historical chronicles and the lake records, we  
454 observe that the ranges of flood-frequency values are similar, i.e. between 0 and around 4  
455 floods per 11 years. We also observe strong similarities in the two flood records with common  
456 periods of low flood frequency in AD 1750-1785, 1820-1860 and 1910-1945 and common  
457 periods of high flood frequency in AD 1785-1820, AD 1945-1970 and AD 1985-2000. Only a  
458 slight time lag (~5 years) appears for the latter period in the lake record. Overall, there is then  
459 good agreement with the historical data, supporting that Lake Foréant sediments record the  
460 variability of past flood events that impacted societies over the last 250 years relatively well.  
461 A major inconsistency, however, appears from 1860 to 1910 since numerous floods are  
462 documented in the lake record but there is missing evidence for flood in the historical record.  
463 A high hydrological activity is documented for the region at this time (e.g. Miramont et al.,  
464 1998; Sivan et al., 2010; Wilhelm et al., 2012a; 2015), suggesting that this may result of a  
465 historical database locally incomplete.

466

### 467 **5.2.2. Potential influences of environmental changes**

468 The Foréant flood record may be considered as relevant over the entire studied period if  
469 erosion processes are stable over time. Erosion processes in the **Foréant catchment** may be  
470 affected by modifications in the river system and/or by land-use changes.

471 The main inflow, the Bouchouse stream, has built an **alluvial** plain upstream the lake where it  
472 is divided in two main meandering branches. An alternate activity of these branches during  
473 floods may disturb the **flood** record by triggering variable sediment dispersion within the lake  
474 basin (e.g. Wilhelm et al., 2015). However, such processes seem to be unlikely because the  
475 stratigraphic correlation highlights a stable pattern of the flood-sediment deposition with the  
476 thickest **FILs** in cores FOR13P2 and FOR13P4 from the depocenter and a thinning of the **FIL**  
477 deposits toward cores FOR13P1 and FOR13P3 located in the slopes (Fig. 2). The **alluvial**  
478 plain may also disturb the record by acting as a sediment trap. Indeed, the meandering river  
479 morphology and the gentle slope of the **alluvial** plain may trigger a decrease of the discharge  
480 velocity, resulting in the deposition of the coarser particles on the plain before entering the

481 lake. This may explain the small variability in grain-size in the Foréant sediment record. The  
482 grain-size ratio between the base (coarser fraction) and the top (finer fraction) of the FILs is  
483 ~1.3, while it usually ranges from 5 to 15 in many different geological and environmental  
484 settings (e.g. Oslegger et al., 2009; Giguet-Covex et al., 2012; Simmoneau et al., 2013;  
485 Wilhelm et al., 2013 Amman et al., 2015; Wilhelm et al., 2015). However, fine particles (i.e.  
486 clays and fine silts that composed the FILs) are transported by suspension in the river (e.g.  
487 Passega, 1964). As a result, their trapping and storage in the alluvial plain is unlikely. A  
488 negligible storage effect on the fine fraction is also supported by the relatively stable  
489 sedimentation rate of the silty sedimentary background (Fig. 6) that suggests an uninterrupted  
490 sediment transport to the lake over the studied period.

491 Erosion processes in the catchment may also be modified by land-use that mainly corresponds  
492 at this altitude to changes in grazing intensity. An increase of grazing intensity may make  
493 soils more vulnerable to erosion during heavy rainfalls and, thereby, may induce an increased  
494 sensitivity of the catchment-lake system to record floods, i.e. higher flood frequency and/or  
495 flood-sediment accumulation in the sediment record (e.g. Giguet-Covex et al., 2012).  
496 Abundance of *Sporormiella* is assumed to reflect local changes of grazing intensity in Lake  
497 Foréant catchment (e.g. Etienne et al., 2013). The concentration of *Sporormiella* ascospores  
498 measured in core FOR13P3 oscillated from 5 to 43 number.cm<sup>-3</sup> through the sequence (Fig.  
499 2), resulting in accumulation rates varying from 12 to 340 number.cm<sup>2</sup>.yr<sup>-1</sup> over time (Fig. 8).  
500 This variability in *Sporormiella* abundance has been compared to the variability in flood  
501 frequency and flood-sediment accumulation (see Supplementary Material). We do not find  
502 significant relationships ( $p > 0.05$ ) between these parameters (Fig. S3), suggesting that  
503 variations in pastoralism seemingly have not had a significant impact on erosion processes in  
504 the Foréant catchment. However, two samples covering the period AD 1734-1760 show both  
505 high *Sporormiella* accumulation rates and flood frequencies (Fig. 8 and S3). This suggests  
506 that the flood frequency during this period may be exacerbated by a punctual and very high  
507 grazing intensity. Hence, we postulate that erosion processes did not change drastically over  
508 the studied period, implying that climate is likely the main factor explaining the recorded  
509 flood activity, with exception of the period AD 1734-1760.

510

### 511 **5.2.3. Palaeoflood activity in the regional climatic setting**

512 Comparison with the historical record shows that the past flood variability is well reproduced  
513 by the Foréant record (Fig. 7). The Foréant palaeoflood record is thus interpreted as the  
514 recurrence of summer-to-autumn flood events triggered by both local and mesoscale  
515 convective phenomena.

516 To discuss the millennium-long flood variability in regard to both Atlantic and Mediterranean  
517 climatic influences in the Alpine domain, the Foréant palaeoflood record is compared to the  
518 palaeoflood records of Lakes Blanc and Allos (Fig. 7 and 8). Lakes Blanc and Allos have  
519 similar characteristics to Lake Foréant such as the high altitude (> 2000 m a.s.l.), the small  
520 catchment area (< 3 km<sup>2</sup>) and the steep catchment slopes, making possible the comparison.  
521 Lake Blanc sediments located in the northern French Alps mainly record Atlantic-sourced  
522 weather pattern of high altitude, i.e. summer local convective events (Fig. 1; Giguet-Covex et  
523 al., 2012; Wilhelm et al., 2012b, 2013). In contrast, Lake Allos sediments located in the  
524 southern French Alps mainly record Mediterranean-sourced weather patterns of high altitude,  
525 i.e. mesoscale convective events (Fig. 1; Wilhelm et al., 2012a, 2015). The last millennium is  
526 usually divided in three climatic periods according to the temperature variations; the warm  
527 Medieval Climate Anomaly (MCA, ca. AD 950-1250), the cold Little Ice Age (LIA, ca. AD  
528 1300-1900) and the warmer 20<sup>th</sup> century (e.g. Lamb, 1965; Büntgen et al., 2011; Luterbacher  
529 et al., 2012 and references therein). During the MCA, the Foréant flood record shows a low  
530 flood frequency with ~10 floods per century and, 4 occurrences of thick flood deposits (> 8  
531 mm thick) that we interpret as high-intensity flood events. During the LIA, the Foréant record  
532 shows a higher flood frequency with ~17 floods per century and only 2 high-intensity events.  
533 The 20<sup>th</sup> century is finally characterized by ~17 floods per century and absence of high-  
534 intensity events. The increased flood frequency during the long and cold period of the LIA,  
535 compared to the MCA, was also observed in the Blanc and Allos records (Wilhelm et al.,  
536 2012a; 2013; Fig. 8), as well as in many other records from the European Alps (e.g. Arnaud et  
537 al., 2012; Glur et al., 2013; Swierczynski et al., 2013; Wirth et al., 2013a, 2013b; Amann et  
538 al., 2015; Schulte et al., 2015) and the north-western Mediterranean area (e.g. Jorda and  
539 Provansal, 1996; Camuffo and Enzi, 1995; Jorda et al., 2002; Thorndycraft and Benito, 2006;  
540 Moreno et al., 2008; Benito et al., 2015; Arnaud-Fassetta et al., 2010). This common pattern  
541 in many flood records of southern Europe may be the result of a southward shift and an  
542 intensification of the dominant westerly winds during boreal summer related to an increase in  
543 the thermal gradient between low (warming) and high (cooling) latitudes (e.g. Bengtsson and

544 Hodges, 2006; Raible et al., 2007). In this scenario, the Alps are likely to experience an  
545 increase in precipitation due to an increase in moisture advection from the North Atlantic. In  
546 contrary, the occurrence of high-intense floods during both the MCA and the LIA periods is a  
547 new feature of Alpine regional patterns, since the most intense floods occurred exclusively  
548 during the MCA in the Blanc record (Wilhelm et al., 2013) or during the LIA in the Allos  
549 record (Wilhelm et al., 2012a; Fig. 8) and other Mediterranean records of the Alpine region  
550 (Jorda and Provansal, 1996; Miramont et al., 1998; Jorda et al., 2002; Arnaud-Fassetta et al.,  
551 2010). This suggests that hydro-meteorological processes related to the Atlantic and to the  
552 Mediterranean climatic influences may alternatively trigger high intense events in the Foréant  
553 area during the MCA and the LIA, respectively. However, the most intense floods at Foréant  
554 appear 3 times more frequent during the MCA than during the LIA, a trend that remains true  
555 when considering various thickness thresholds (8, 7, 6 or 5 mm) for high-intensity flood  
556 events. In addition, the mean sediment accumulation per flood event shows values ~50%  
557 higher during the MCA than during the LIA (3.8 vs. 2.4 mm/flood), suggesting an increase of  
558 the mean flood-event intensity during the warmer period. These two evidences of increased  
559 flood intensity during the warm period may be related to the strengthening of local convective  
560 processes due to higher temperatures, as suggested for the north-western flood pattern  
561 (Giguët-Covex et al., 2012; Wilhelm et al., 2012b, 2013). In the Foréant area, higher  
562 temperatures seem thus to result in a lower flood frequency but in higher flood intensity on  
563 the multi-centennial time scale. Flood frequency and intensity during the warmer 20<sup>th</sup> century,  
564 however, do not follow these trends. The frequency is still similar to the LIA one and high-  
565 intense events are absent and the mean sediment accumulation per flood event (2.2 mm/flood)  
566 is also similar to the LIA. Two hypotheses may be considered to explain this ‘anomaly’. First,  
567 this may result from the relatively short period covered by the 20<sup>th</sup> century (i.e. ~100 years) in  
568 comparison with the multi-centennial variability documented for the MCA (i.e. ~300 years)  
569 and the LIA (i.e. ~600 years) periods. Thereby, considering stable temperature-flood  
570 relationships over time, the 20<sup>th</sup> century might be a transitional period toward a MCA-like  
571 flood pattern with the global warming. This latter possibility would imply an increasing flood  
572 hazard in the Foréant region in a near future due to an increased occurrence of high-intensity  
573 flood events. Secondly, this may also result from a non-linearity of the flood response to  
574 temperature, making the analogy between the MCA and the 20<sup>th</sup> century more complex, in  
575 particular as the current warming is caused by an unprecedented forcing (greenhouse gases).  
576 Moreover, the other external forcing such as solar activity, and volcanic eruptions largely  
577 varied over the last millennium (e.g. Servonnat et al., 2010; Delaygue et Bard, 2011; Gao et

578 al., 2012; Crowley and Unterman, 2013) and their non-linear combination also with the  
579 greenhouse gases may result in different time-space temperature patterns and, thereby, in  
580 different flood responses during these two periods. In order to explore forcing-dependent  
581 impacts on the climate-flood relationships, deeper analysis utilizing for example advanced  
582 statistics or simulations is required.

583

## 584 **6. Conclusion**

585 High-resolution sedimentological and geochemical analyses of the Lake Foréant sequence  
586 revealed 171 **event layers**. Three of the 171 **event layers** can be differentiated by characteristic  
587 geochemical features (high Ca contents and low Mn contents) and stratigraphic succession.  
588 These **three event layers** are interpreted as mass-movement-induced layers. The other 168  
589 **event layers** show a geochemical pattern similar to the sedimentary background that mainly  
590 corresponds to detrital material sourced by the rivers. These **event layers** are interpreted as  
591 flood-induced **layers**. Only small changes in grain-size variability in the flood-induced **layers**  
592 precluded the use of the grain size as a flood-intensity proxy. However, the relatively  
593 homogeneous **grain size and** deposition pattern within the lake basin made the flood-deposit  
594 thickness a suitable proxy for the reconstruction of flood intensity.

595 Comparison with local historical data indicates that Foréant sediments sensitively record past  
596 flood events with variability in frequency and intensity related to both Atlantic- and  
597 Mediterranean-influenced hydro-meteorological processes, i.e. local and mesoscale  
598 convective systems occurring from late spring to fall. As there is no evidence of major  
599 changes in erosion processes due to landscape evolution or grazing **intensity** (except maybe  
600 for the period AD 1734-1760), we assume that climate and not land-use changes exerts the  
601 dominant control on flood variability in the Foréant-record over the past millennium. The  
602 comparison to northern and southern flood records, i.e. to Atlantic- and Mediterranean-  
603 influenced records, highlights that the increase of flood frequency during the cold period of  
604 the LIA is a common feature of all regional flood patterns from the European Alps. The  
605 comparison also revealed that high-intensity events in the Foréant region occurred during both  
606 the cold LIA and the warm MCA periods. This specific feature of the Foréant flood record  
607 likely results from its sensitivity to both Atlantic and Mediterranean climatic influences.  
608 However, high-intensity events are more frequent and the flood intensity is higher during the  
609 warm MCA. This suggests that flood hazard may increase in the Foréant region in response to

610 global warming. Surprisingly, the flood variability over the warm 20<sup>th</sup> century appears still  
611 similar to the flood variability of the cold LIA period. This 20<sup>th</sup>-century flood trend may be  
612 interpreted as the result of a transitional period toward a MCA-like flood pattern. This would  
613 imply an increasing flood hazard in the Foréant region in a near future due to more frequent  
614 high-intensity flood events. However, this may also result from a non-linear temperature-  
615 flood relationship. In order to better understand the underlying mechanisms deeper analyses  
616 employing advanced statistics or simulations need to be applied.

617

## 618 **Acknowledgments**

619 B. Wilhelm's post-doctoral fellowship (2013-2014) was supported by a grant from the AXA  
620 Research Fund. We would also like to thank Pierre Sabatier for his help with analysis of the  
621 <sup>210</sup>Pb data, Anne-Lise Develle for fruitful discussions, Petra Boltshauser-Kaltenrieder for help  
622 with identification of terrestrial-plant remains prior to <sup>14</sup>C dating and Nicolas Thouveny and  
623 François Demory for providing access to facilities at the CEREGE palaeomagnetic laboratory  
624 (Aix-Marseille University) and for fruitful discussions.

625

626

627

## 628 **References**

629 Amann, B., Sönke, S., Grosjean, M.: A millennial-long record of warm season precipitation  
630 and flood frequency for the North-western Alps inferred from varved lake sediments:  
631 implications for the future, *Quaternary Science Reviews*, 115, 89-100, 2015.

632 Appleby, P.G., Richardson, N., Nolan, P.J.: <sup>241</sup>Am dating of lake sediments, *Hydrobiologia*,  
633 214, 35–42, 1991.

634 Arnaud, F., Lignier, V., Revel, M., Desmet, M., Pourchet, M., Beck, C., Charlet, F.,  
635 Trentesaux, A., Tribouvillard, N.: Flood and earthquake disturbance of <sup>210</sup>Pb geochronology  
636 (Lake Anterne, North French Alps), *Terra Nova*, 14, 225–232, 2002.

637 Arnaud, F., Révillon, S., Debret, M., Revel, M., Chapron, E., Jacob, J., Giguex-Covex, C.,  
638 Poulénard, J., Magny, M.: Lake Bourget regional erosion patterns reconstruction reveals

639 Holocene NW European Alps soil evolution and paleohydrology, *Quaternary Science*  
640 *Reviews*, 51, 81–92, 2012.

641 Arnaud-Fassetta, G., and Fort, M.: Respective parts of hydroclimatic and anthropic factors in  
642 the recent evolution (1956-2000) of the active channel of the Upper Guil, Queyras, Southern  
643 French Alps, *Méditerranée*, 102, 143-156, 2004.

644 Arnaud-Fassetta, G., Carcaud, N., Castanet, C. and Salvador, P.G.: Fluvial  
645 palaeoenvironments in archaeological context: geographical position, methodological  
646 approach and global change—hydrological risk issues, *Quat. Int.*, 216, 93–117, 2010.

647 Avşar, U., Hubert-Ferrari, A., De Batist, M., Lepoint, G., Schmidt S. and Fagel N.:  
648 Seismically-triggered organic-rich layers in recent sediments from Göllüköy Lake (North  
649 Anatolian Fault, Turkey), *Quat. Sci. Rev.*, 103, 67–80, 2014.

650 Barletta, F., St-Onge, G., Channell, J.E.T. and Rochon, A.: Dating of Holocene western  
651 Canadian Arctic sediments by matching paleomagnetic secular variation to a geomagnetic  
652 field model, *Quaternary Science Reviews*, 29, 2315–2324, 2010.

653 Bengtsson, L., and Hodges, K.I.: Storm tracks and climate change, *Journal of Climate*, 19,  
654 3518–3543, 2006.

655 Beniston, M. and Stephenson, D.B.: Extreme climatic events and their evolution under  
656 changing climatic conditions, *Glob Planet Change*, 44, 1–9, 2004.

657 Benito, G., Macklin, M.G., Zielhofer, C., Jones A., and Machado, M.J.: Holocene flooding  
658 and climate change in the Mediterranean, *Catena*, 130, 13-33, 2015.

659 Blaauw, M.: Methods and code for ‘classical’ age modelling of radiocarbon sequences, *Quat.*  
660 *Geochronol.*, 5, 512–518, 2010.

661 Bloemendal, J., King, J.W., Hall, F.R. and Doh, S.-J.: Rock magnetism of Late Neogene and  
662 Pleistocene deep-sea sediments relationship to sediment source, diagenetic processes, and  
663 sediment lithology, *Journal of Geophysical Research*, 97: 4361-4375, 1992.

664 Boudevillain, B., Argence, S., Claud, C., Ducrocq, V., Joly, B., Lambert, D., Nuissier, O.,  
665 Plu, M., Ricard, D., Arbogast, P., Berne, A., Chaboureaud, J.P., Chapon, B., Crepin, F.,  
666 Delrieu, G., Doerflinger, E., Funatsu, B.M., Kirstetter, P.E., Masson, F., Maynard, K.,  
667 Richard, E., Sanchez, E., Terray, L. and Walpersdorf, A.: Cyclogenesis et précipitations  
668 intenses en région méditerranéenne: origines et caractéristiques, *La Meteorol.*, 66, 18–28,  
669 2009.

670 Boroneant, C., Plaut, G., Giorgi, F. and Bi., X.: Extreme precipitation over the Maritime Alps  
671 and associated weather regimes simulated by a regional climate model: Present-day and future  
672 climate scenarios, *Theor. Appl. Climatol.*, 86, 81–99, 2006.

673 Büntgen, U., Tegel, W., Nicolussi, K., McCormick, M., Frank, D., Trouet, V., Kaplan, J.,  
674 Herzig, F., Heussner, U., Wanner, H., Luterbacher, J., Esper, J. : 2500 years of European  
675 climate variability and human susceptibility, *Science*, 331, 578-582, 2011

676 Buzzi, A. and Foschini, L.: Mesoscale meteorological features associated with heavy  
677 precipitation in the Southern Alpine Region, *Meteorol. Atmos. Phys.*, 72, 131–146, 2000.

678 Campbell, C.: Late Holocene lake sedimentology and climate change in southern Alberta,  
679 Canada, *Quatern. Res.*, 49, 96–101, 1998.

680 Camuffo, D. and Enzi, S.: The analysis of two bi-millenary series: Tiber and Po River Floods,  
681 In: Jones, P.D. Bradley, R.S. Jouzel, J. (Eds.), *Climatic Variations and Forcing Mechanisms*  
682 of the Last 2000 years, NATO ASI Series, Series I: Global Environmental Change, 41  
683 Springer, Stuttgart, 433–450, 1995.

684 Corella, J.P., Benito, G., Rodriguez-Lloveras, X., Brauer, A. and Valero-Garcès, B.L.:  
685 Annually-resolved lake record of extreme hydro-meteorological events since AD 1347 in NE  
686 Iberian Peninsula, *Quat. Sci. Rev.*, 93, 77-90, 2014.

687 Croudace, I.W., Rindby, A. and Rothwell, R.G.: ITRAX: description and evaluation of a new  
688 multi-function X-ray core scanner. In: Rothwell, R.G. (Ed.), *New Techniques in Sediment*  
689 *Core Analysis*, Geological Society, London, Special Publications, 367, 51-63, 2006.

690 Crowley, T.J. and Untermann, M.B.: Technical details concerning development of a 1200-yr  
691 proxy index for global volcanism, *Earth Syst. Sci. Data*, 5, 187-197, 2013.

692 Cuvén, S., Francus, P. and Lamoureux, S.: Estimation of grain size variability with micro X-  
693 ray fluorescence in laminated lacustrine sediments, Cape Bounty, Canadian High Arctic,  
694 *Journal of Paleolimnology*, 44, 803–817, 2010.

695 Czymzik, M., Brauer, A., Dulski, P., Plessen, B., Naumann, R., von Grafenstein, U. and  
696 Scheffler, R.: Orbital and solar forcing of shifts in Mid- to Late Holocene flood intensity from  
697 varved sediments of pre-alpine Lake Ammersee (southern Germany), *Quatern. Sci. Rev.*, 61,  
698 96–110, 2013.

699 Davis, O.K. and Schafer, D.: *Sporormiella* fungal spores, a palynological means of detecting  
700 herbivore density. *Palaeogeog., Palaeoclimatol., Palaeoecol.*, 237, 40–50, 2006.

701 Davison, W.: Iron and manganese in lakes, *Earth-Science Reviews*, 34, 119-163,1993

702 Deflandre, B., Mucci, A., Gagne, J.P., Guignard, C., Sundby, B.: Early diagenetic processes  
703 in coastal marine sediments disturbed by a catastrophic sedimentation event, *Geochimica et*  
704 *Cosmochimica Acta*, 66(14), 2547–2558, 2002.

705 Delaygue, G. and Bard, E.: An Antarctic view of Beryllium-10 and solar activity for the past  
706 millennium, *Climate Dynamics*, 36, 2201–2218, 2011.

707 Donadini, F., M. Korte, Constable C. G.: Geomagnetic field for 0–3 ka: 1. New data sets for  
708 global modeling, *Geochemistry Geophysics Geosystems (G3)*, 10, Q06007,  
709 doi:10.1029/2008GC002295, 2009.

710 Durant, Y., Laternser, M., Giraud, G., Etchevers, P., Lesaffre, B., Merindol, L.: Reanalysis of  
711 44 Yr of Climate in the French Alps (1958–2002): Methodology, Model Validation,  
712 Climatology, and Trends for Air Temperature and Precipitation, *J. Applied Meteorology and*  
713 *Climatology*, 48(3):429-449, 2009.

714 Etienne, D., Wilhelm, B., Sabatier, P., Reyss, J.L. and Arnaud, F.: Influence of sample  
715 location and livestock numbers on *Sporormiella* concentrations and accumulation rates in  
716 surface sediments of Lake Allos, French Alps, *J. Paleolimnol.*, 49, 117–127, 2013.

717 Etienne, D. and Jouffroy-Bapicot, I.: Optimal counting limit for fungal spore abundance  
718 estimation using *Sporormiella* as a case study. *Veget. Hist. Archaeobot*, 23, 743-749, 2014.

719 Faegri, K. and Iversen, J.: *Textbook of Pollen Analysis*. John Wiley & Sons, New York. 328,  
720 1989.

721 Frei, C., Schöll, R., Fukutome, S., Schmidli, J., Vidale, P.L.: Future change of precipitation  
722 extremes in Europe: Intercomparison of scenarios from regional climate models, *J. Geophys.*  
723 *Res. Atm.*, 111, D06105. doi:10.1029/2005JD005965, 2006.

724 Gao, C., Robock, A. and Ammann, C.: Volcanic forcing of climate over the past 1500 years:  
725 An improved ice core-based index for climate models, *J. Geophys. Res.*, 113, D23111, 2008.

726 Giguet-Covex, C., Arnaud, F., Enters, D., Poulénard, J., Millet, L., Francus, P., David, F.,  
727 Rey, P.J., Wilhelm, B. and Delannoy, J.J.: Frequency and intensity of high altitude floods  
728 over the last 3.5 ka in NW European Alps, *Quatern. Res.*, 77, 12–22, 2012.

729 Gilli, A., Anselmetti, F.S., Glur, L. and Wirth, S.B.: Lake sediments as archives of recurrence  
730 rates and intensities of past flood events, In: *Dating Torrential Processes on Fans and Cones –*

731 Methods and Their Application for Hazard and Risk Assessment (Eds M. Schneuwly-  
732 Bollschweiler, M. Stoffel and F. Rudolf-Miklau), *Adv. Global Change Res.* 47, 225–242,  
733 2012.

734 Girardclos, S., Schmidt, O.T., Sturm, M. , Ariztegui, D., Pugin A., and Anselmetti F.S.: The  
735 1996 AD delta collapse and large turbidite in Lake Brienz, *Marine Geology*, 24, 137–154,  
736 2007.

737 Glur, L., Wirth, S.B., B€untgen, U., Gilli, A., Haug, G.H., Schär, C., Beer, J. and Anselmetti,  
738 F.S., Frequent floods in the European Alps coincide with cooler periods of the past 2500  
739 years, *Sci. Rep.*, 3, 2770, 2013.

740 Goldberg, E.D.: *Geochronology with 210Pb Radioactive Dating*, IAEA, Vienna, 121–131.  
741 1963

742 Gottardi, F., Obled, C., Gailhard, J., Paquet, E.: Statistical reanalysis of precipitation fields  
743 based on ground network data and weather patterns: Application over French mountains, *J.*  
744 *Hydrology*, 432–433, 154–167, 2010.

745 Howarth, J.D., Fitzsimons, S.J., Norris, R.J. and Jacobsen, G.E.: Lake sediments record high  
746 intensity shaking that provides insight into the location and rupture length of large  
747 earthquakes on the Alpine Fault, New Zealand, *Earth and Planetary Science Letters*, 403,  
748 340–351, 2014.

749 IPCC: *The Physical Science Basis. Contribution of Working Group I to the Fifth Assessment*  
750 *Report of the Intergovernmental Panel on Climate Change* (Eds T.F. Stocker, D. Qin, G.-K.  
751 Plattner, M. Tignor, S.K. Allen, J. Boschung, A. Nauels, Y. Xia, V. Bex and P.M. Midgley).  
752 Cambridge University Press, Cambridge, United Kingdom and New York, NY, USA, 2013

753 Jorda, M. and Provansal, M.: Impact de l’anthropisation et du climat sur le detritisme en  
754 France du sud-est (Alpes du Sud et Provence), *Bulletin de la Societe Geologique de France*,  
755 167, 159–168 ,1996.

756 Jorda, M., Miramont, C., Rosique, T. and Sivan, O.: Evolution de l’hydrosysteme durancien  
757 (Alpes du Sud, France) depuis la fin du Pleniglaciaire superieur, In: Bravard, J.-P., Magny, M.  
758 (Eds.), *Les Fleuves ont une Histoire, Paleo-environnement des Rivieres et des lacs Francais*  
759 *depuis 15000 ans. Errance, Paris*, 239–249, 2002.

760 Jenny, J.-P., Wilhelm, B., Arnaud, F., Sabatier, P., Giguet-Covex, C., Mélo, A., Fanget, B.,  
761 Malet, E., Ployon, E. and Perga, M.E., A 4D sedimentological approach to reconstructing the

762 flood frequency and intensity of the Rhône River (Lake Bourget, NW European Alps), J.  
763 Paleolimnol., 51, 469–483, 2014.

764 Korte, M., Donadini, F., Constable, C.G. : Geomagnetic field for 0–3 ka: 2. A new series of  
765 time-varying global models, *Geochemistry Geophysics Geosystems (G3)*, 10, Q06008, doi:  
766 10.1029/2008GC002297, 2009.

767 Lamb, H. H.: The early medieval warm epoch and its sequel, *Palaeogeogr. Palaeoclimatol.*  
768 *Palaeoecol.*, 1, 13–37, 1965.

769 Lambert, J, and Levret-Albaret, A.: Mille ans de séismes en France. Catalogues d'épicentres,  
770 paramètres et references, Ouest-Editions, Presses Académiques, Nantes. 1996.

771 Lapointe, F., Francus, P., Lamoureaux, S.F., Saïd, M. and Cuven, S.: 1,750 years of large  
772 rainfall events inferred from particle size at East Lake, Cape Bounty, Melville Island, Canada,  
773 *Journal of Paleolimnology*, 48(1), 159–173, 2012.

774 Lionello, P., Abrantes, F., Congedi, L., Dulac, F., Gacic, M., Gomis, D., Goodess, C., Hoff,  
775 H., Kutiel, H., Luterbacher, J., Planton, S., Reale, M., Schröder, K., Struglia, M.V., Toreti, A.,  
776 Tsimplis, M., Ulbrich, U. and Xoplaki, E.: Introduction: Mediterranean Climate: Background  
777 Information in Lionello P. (Ed.) *The Climate of the Mediterranean Region. From the Past to*  
778 *the Future*, Amsterdam: Elsevier (Netherlands), XXXV-IXXX, 2012.

779 Lurcock, P. C. and Wilson, G. S.: PuffinPlot: A versatile, user-friendly program for  
780 paleomagnetic analysis, *Geochemistry, Geophysics, Geosystems*, 13, Q06Z45, 2012.

781 Luterbacher, J., García-Herrera, R., Akcer-On, S., Allan, R., Alvarez-Castro, M. C., Benito,  
782 G., Booth, J., Büntgen, U., Cagatay, N., Colombaroli, D., Davis, B., Esper, J., Felis, T.,  
783 Fleitmann, D., Frank, D., Gallego, D., Garcia-Bustamante, E., Glaser, R., González-Rouco,  
784 J.F., Goosse, H., Kiefer, T., Macklin, M.G., Manning, S., Montagna, P., Newman, L., Power,  
785 M.J., Rath, V., Ribera, P., Riemann, D., Roberts, N., Sicre, M., Silenzi, S., Tinner, W.,  
786 Valero-Garces, B., van der Schrier, G., Tzedakis, C., Vannièrè, B., Vogt, S., Wanner, H.,  
787 Werner, J.P., Willett, G., Williams, M.H., Xoplaki, E., Zerefos, C.S. and Zorita, E.: A review  
788 of 2000 years of paleoclimatic evidence in the Mediterranean, In: Lionello, P. (Ed.), *The*  
789 *Climate of the Mediterranean region: from the past to the future*, Elsevier, Amsterdam, The  
790 Netherlands, 87-185, 2012.

791 Miramont, C., Jorda, M. and Pichard, G.: Évolution historique de la morphogenèse et de la  
792 dynamique fluviale d'une rivière méditerranéenne : l'exemple de la moyenne Durance  
793 (France du sud-est), *Géographie physique et Quaternaire*, 52(3), 381-392, 1998.

794 Moernaut, J., M. De Batist, F. Charlet, K. Heirman, E. Chapron, M. Pino, R. Brümmer and R.  
795 Urrutia, Giant earthquakes in South-Central Chile revealed by Holocene mass-wasting events  
796 in Lake Puyehue, *Sediment. Geol.*, 195, 239–256, 2007.

797 Moernaut, J., Van Daele, M., Heirman, K., Fontijn, K., Strasser, M., Pino, M., Urrutia R., and  
798 De Batist, M.: Lacustrine turbidites as a tool for quantitative earthquake reconstruction: New  
799 evidence for a variable rupture mode in south central Chile, *J. Geophys. Res. Solid Earth*,  
800 119, doi:10.1002/2013JB010738, 2014.

801 Monecke, K., Anselmetti, F.S., Becker, A., Sturm, M. and Giardini, D.: The record of historic  
802 earthquakes in lake sediments of Central Switzerland, *Tectonophysics*, 394, 21–40, 2004.

803 Munich Re Group: Annual Review: Natural Catastrophes 2002, Munich Re Group, Munich,  
804 Germany, 2003.

805 Moreno, A., Valero-Garces, B.L., Gonzalez-Samperiz, P. and Rico, M.: Flood response to  
806 rainfall variability during the last 2000 years inferred from the Taravilla Lake record (Central  
807 Iberian Range, Spain), *J. Palaeolimnol.*, 40, 943–961, 2008.

808 Noren, A.J., Bierman, P.R., Steig, E.J., Lini, A. and Southon, J.: Millennial-scale storminess  
809 variability in the northeastern United States during the Holocene epoch, *Nature*, 419, 821-824,  
810 2002.

811 Osleger, D.A., Heyvaert, A.C., Stoner, J.S. and Verosub, K.L.: Lacustrine turbidites as  
812 indicators of Holocene storminess and climate: Lake Tahoe, California and Nevada, *J*  
813 *Paleolimnol.*, 42:103–122, 2009.

814 Page, M.J., Trustrum, N.A. and DeRose, R.C.: A high resolution record of storm-induced  
815 erosion from lake sediments, New Zealand, *Journal of Paleolimnology*, 11, 333-348, 1994.

816 Parajka, J., Kohnová, S., Bálint, G., Barbuc, M., Borga, M., Claps, P., Cheval, S., Dumitrescu,  
817 A., Gaume, E., Hlavčová, K., Merz, R., Pfaundler, M., Stancalie, G., Szolgay, J., Blöschl, G.:  
818 Seasonal characteristics of flood regimes across the Alpine–Carpathian range, *J. of*  
819 *Hydrology*, 394,78–89, 2010.

820 Passega, R.: Grain-size representation by CM patterns as a geological tool, *J. of Sedimentary*  
821 *Petrology*, 34(4), 830–847, 1964.

822 Plaut, G., Schuepbach, E. and Doctor, M. Heavy precipitation events over a few Alpine sub-  
823 regions and the links with large-scale circulation, 1971–1995, *Climate Research*, 17, 285–302,  
824 2009.

825 Raible, C.C., Yoshimori, M., Stocker, T.F. and Casty, C.: Extreme midlatitude cyclones and  
826 their implications for precipitation and wind speed extremes in simulations of the Maunder  
827 Minimum versus present day conditions. *Clim. Dyn.* 28, 409–423, 2007.

828 Rajczak, J., Pall, P. and Schär, C.: Projections of extreme precipitation events in regional  
829 climate simulations for Europe and the Alpine Region, *J. Geophys. Res. Atm.*, 118, 1–17,  
830 2013.

831 Reimer, P.J., Bard, E., Bayliss, A., Beck, J.W., Blackwell, P.G., Bronk Ramsey, C., Buck,  
832 C.E., Cheng, H., Edwards, R.L., Friedrich, M., Grootes, P.M., Guilderson, T.P., Haflidason,  
833 H., Hajdas, I., Hatt, C., Heaton, T.J., Hogg, A.G., Hughen, K.A., Kaiser, K.F., Kromer, B.,  
834 Manning, S.W., Niu, M., Reimer, R.W., Richards, D.A., Scott, E.M., Southon, J.R., Turney,  
835 C.S.M. and van der Plicht, J.: IntCal13 and MARINE13 radiocarbon age calibration curves 0-  
836 50000 years calBP, *Radiocarbon*, 55(4), 1869–1887, 2013.

837 Sauerbrey, M. A., Juschus, O., Gebhardt, A. C., Wennrich, V., Nowaczyk, N. R. and Melles,  
838 M.: Mass movement deposits in the 3.6Ma sediment record of Lake Elgygytgyn, Far East  
839 Russian Arctic, *Climate of the Past* 9, 1949–1967, 2013.

840 Schiefer, E., Gilbert, R. and Hassan, M.A.: A lake sediment-based proxy of floods in the  
841 Rocky Mountain Front Ranges, Canada, *Journal of Paleolimnology*, 45, 137–149, 2011.

842 Schulte, L., Peña, J.C., Carvalho, F., Schmidt, T., Julià, R., Llorca, J. and Veit, H.: A 2600-  
843 year history of floods in the Bernese Alps, Switzerland: frequencies, mechanisms and climate  
844 forcing, *Hydrol. Earth Syst. Sci.*, 19, 3047–3072, 2015.

845 Schwartz, S., Tricart, P., Lardeaux, J.M., Guillot, S. and Vidal, O.: Late tectonic and  
846 metamorphic evolution of the Piedmont accretionary wedge (Queyras Schistes lustrés, western  
847 Alps): Evidences for tilting during Alpine collision, *Geol. Soc. Ame. Bull.*, 121, 502-518,  
848 2009.

849 Scotti, O., Baumont, D., Quenet, G. and Levret, A.: The French macroseismic database  
850 SISFRANCE: objectives, results and perspectives, *Annals of Geophysics*, 47(2), 571-581,  
851 2004.

852 Servonnat, J., Yiou, P., Khodri, M., Swingedouw, D., Denvil, S.: Influence of solar  
853 variability, CO<sub>2</sub> and orbital forcing during the last millennium in the IPSLCM4 model, *Clim.*  
854 *Past*, 6, 445-460, 2010.

855 Simonneau, A., Chapron, E., Vanni re, B., Wirth, S.B., Gilli, A., Giovanni, C. Di.,  
856 Anselmetti, F. S., Desmet, M. and Magny M.: Mass-movement and flood-induced deposits in  
857 Lake Ledro, southern Alps, Italy: implications for Holocene palaeohydrology and natural  
858 hazards, *Clim. Past* 9, 825-840, 2013.

859 Sivan, O., Miramont, C., Pichard, G. and Prosper-Laget, V. : Les conditions climatiques de la  
860 torrentialit  au cours du Petit Age Glaciaire de Provence, *Archeologie du Midi Medieval*, 26,  
861 157–168, 2009.

862 Stockmarr, J.: Tablets with spores used in absolute pollen analysis. *Pollen Spores* 13, 615–  
863 621, 1971.

864 St ren, E.N., Olaf Dahl, S., Nesje, A. and Paasche  .: Identifying the sedimentary imprint of  
865 high-frequency Holocene river floods in lake sediments: development and application of a  
866 new method, *Quat. Sci. Rev.*, 29, 3021-3033, 2010.

867 Strasser, M., Hilbe, M. and Anselmetti, F.S.: Mapping basin-wide subaquatic slope failure  
868 susceptibility as a tool to assess regional seismic and tsunami hazards, *Mar. Geophys. Res.*,  
869 32, 331–347, 2011.

870 Sturm, M. and Matter, A.: Turbidites and varves in Lake Brienz (Switzerland): deposition of  
871 clastic detritus by density currents, *Int. Assoc. Sedimentol. Spec. Publ.*, 2, 147–168, 1978.

872 Swierczynski, T., Lauterbach, S., Dulski, P., Delgado, J., Merz, B. and Brauer, A.: Mid- to  
873 late Holocene flood frequency changes in the northeastern Alps as recorded in varved  
874 sediments of Lake Mondsee (Upper Austria), *Quat. Sci. Rev.*, 80, 78–90, 2013.

875 Tachikawa, K., Cartapanis, O., Vidal, L., Beaufort, L., Barlyaeva, T., Bard, E.: The  
876 precession phase of hydrological variability in the Western Pacific Warm Pool during the past  
877 400 ka, *Quat. Sci. Rev.*, 30, 3716–3727, 2011.

878 Thorndycraft, V.R. and Benito, G.: Late Holocene chronology of Spain: the role of climatic  
879 variability and human impact, *Catena*, 66, 34–41, 2006.

880 Torres, N.T., Och, L.M., Hauser, P.C., Furrer, G., Brandl, H., Vologina, E., Sturm, M., and  
881 B rgmann, H. z M ller, B.: Early diagenetic processes generate iron and manganese oxide

882 layers in the sediments of Lake Baikal, Siberia, *Env. Sci.: Processes Impacts*, 16, 879–889,  
883 2014.

884 Trigo, I.F. and Davies, T.D.: Decline in Mediterranean rainfall caused by weakening of  
885 Mediterranean cyclones, *Geophysical Research Letters*, 27(18), 2913–2916, 2000.

886 Van Daele, M., Versteeg, W., Pino, M., Urrutia, R. and De Batist, M.: Widespread  
887 deformation of basin-plain sediments in Aysén fjord [Chile] due to impact by earthquake-  
888 triggered, onshore-generated mass movements, *Marine Geol.*, 337, 67–79, 2013.

889 Van Daele, M., Moernaut, J., Doom, L., Boes, E., Fontijn, K., Heirman, K., Vandoorne, W.,  
890 Hebbeln, D., Pino, M., Urrutia, R., Brümmer, R. and De Batist, M.: A comparison of the  
891 sedimentary records of the 1960 and 2010 great Chilean earthquakes in 17 lakes: Implications  
892 for quantitative lacustrine palaeoseismology, *Sedimentology*, 62(5): 1466–1496, 2015.

893 Van Geel, B. and Aptroot, A.: Fossil ascomycetes in Quaternary deposits. *Nova Hedwig* 82,  
894 313–329, 2006.

895 Van Geel, B., Buurman, J., Brinkkemper, O., Schelvis, J., Aptroot, A., van Reenen, G. and  
896 Hakjebilj, T.: Environmental reconstruction of a Roman period settlement site in Uitgeest (The  
897 Netherlands), with special reference to coprophilous fungi. *J. Archaeol. Sci.* 30, 873–883,  
898 2003.

899 Wilhelm, B., Arnaud, F., Sabatier, P., Crouzet, C., Brisset, E., Chaumillon, E., Disnar, J.R.,  
900 Guiter, F., Malet, E., Reyss, J.L., Tachikawa, K., Bard, E. and Delannoy, J.J.: 1400 years of  
901 extreme precipitation patterns over the Mediterranean French Alps and possible forcing  
902 mechanisms, *Quat. Res.*, 78, 1–12, 2012a.

903 Wilhelm, B., Arnaud, F., Enters, D., Allignol, F., Legaz, A., Magand, O., Revillon, S.,  
904 Giguet-Covex, C. and Malet, E.: Does global warming favour the occurrence of extreme  
905 floods in European Alps? First evidences from a NW Alps proglacial lake sediment record,  
906 *Clim. Change.*, 113, 563–581, 2012b.

907 Wilhelm, B., Arnaud, F., Sabatier, P., Magand, O., Chapron, E., Courp, T., Tachikawa, K.,  
908 Fanget, B., Malet, E., Pignol, C., Bard, E. and Delannoy, J.J.: Palaeoflood activity and climate  
909 change over the last 1400 years recorded by lake sediments in the NW European Alps, *J.*  
910 *Quat. Sci.*, 28, 189–199, 2013.

911 Wilhelm, B., Sabatier, P. and Arnaud, F.: Is a regional flood signal reproducible from lake  
912 sediments? *Sedimentology*, 62(4), 1103–1117. 2015.

913 Wirth S.B., Glur, L., Gilli, A. and Anselmetti, F.S.: Holocene flood frequency across the  
914 Central Alps – solar forcing and evidence for variations in North Atlantic atmospheric  
915 circulation, *Quatern. Sci. Rev.*, 80, 112–128, 2013a.

916 Wirth, S.B., Gilli, A., Simonneau, A., Ariztegui, D., Vannière, B., Glur, L., Chapron, E.,  
917 Magny, M. and Anselmetti, F.S.: A 2000-year long seasonal record of floods in the southern  
918 European Alps. *Geophys. Res. Lett.*, 40(15), 4025-4029, 2013b.

919

920 Table 1. Radiocarbon dates of core FOR13P4. We calculated the event-free sedimentary  
921 depth by removing the graded beds, which were considered to be instantaneous deposits. See  
922 text for explanation, nature of samples and calibration procedures.

923

924 Figure 1. (A) Location of Lake Foréant in the Western Alps, (B) compared to the locations of  
925 the previously studied Lakes Blanc (BLB, Wilhelm et al., 2012b; BAR, Wilhelm et al., 2013)  
926 and Lake Allos (ALO, Wilhelm et al., 2012a). (C) Location of the Foréant catchment area in  
927 the hydrological network flowing to the village of Ristolas. (D) Geological and  
928 geomorphological characteristics of the Foréant catchment area. (E) Bathymetric map of Lake  
929 Foréant and coring sites.

930

931 Figure 2. Lithological descriptions of cores and stratigraphic correlations based on  
932 sedimentary facies. For each core, a photography (left), a X-ray image (center) and a  
933 stratigraphic log is shown (right).  $^{14}\text{C}$  samples are indicated by red stars. Variability in grain-  
934 size distribution and geochemical elements (Fe, K, Ca and Mn) is shown for the core  
935 FOR13P2.  $\text{Mo}_{\text{inc}}$  used as a high-resolution proxy of density is shown close to the density  
936 measurements performed by gamma-ray attenuation. Variability in *Sporomiella* concentration  
937 is shown for core FOR13P3.

938

939 Figure 3. To illustrate the different geochemical characteristics of the sedimentary  
940 background and the graded layers, their Ca intensities were plotted against their Fe, K and Mn  
941 intensities. FIL refers to flood- and MMIL to mass-movement-induced layers. The different  
942 MMILs are labelled according to figure 2.

943

944 Figure 4. (A)  $^{226}\text{Ra}$ ,  $^{210}\text{Pb}$  and  $^{137}\text{Cs}$  profiles for core ALO09P12. (B) Application of a CFCS  
945 model to the event-free sedimentary profile of  $^{210}\text{Pb}$  in excess (without the thick graded beds  
946 considered as instantaneous deposits). (C) Resulting age–depth relationship with  $1\sigma$   
947 uncertainties and locations of the historic  $^{137}\text{Cs}$  peaks supporting the  $^{210}\text{Pb}$ -based ages. C  
948 corresponds to the historic  $^{137}\text{Cs}$  peak of Chernobyl (AD 1986) and MP to the maximum  $^{137}\text{Cs}$   
949 peak of the nuclear fallout (AD 1963).

950

951 Figure 5. (A) Raw declination and inclination profiles of cores FOR13P1, FOR13P2 and  
952 FOR13P4. (B) The same profiles after removal of the thickest graded beds (interpreted as  
953 event layers) and adjustment of the different specific-core depths to a common reference  
954 depth. (C) Average of profiles shown in (B). (D) Correlation to the ARCH3.4k model  
955 reference curve of declination and inclination (Donadini et al., 2009; Korte et al., 2009).  
956 ChRM means characteristic remanent magnetization. The well-correlated declination and  
957 inclination features are labelled D-x and I-x, respectively.

958

959 Figure 6. Age–depth model for core FOR13P2 calculated using the “clam” R-code package,  
960 combining historic  $^{137}\text{Cs}$  peaks,  $^{210}\text{Pb}$  ages, calibrated  $^{14}\text{C}$  ages and magnetic features on the  
961 left side. Probability distribution frequencies of mass-movement ages and possible  
962 correlations to historical earthquakes on the right side.

963

964 Figure 7. Comparison over the last 250 years of the reconstructed Foréant flood frequency  
965 (11-yr running sum) and intensity (thickness of flood deposits) with the frequency (11-yr  
966 running sum) of historical floods at Ristolas. The question mark refers to a possible gap in the  
967 historical data.

968

969 Figure 8. Comparison over the last millennium of (B) the reconstructed Foréant flood  
970 frequency (31-yr running average) and intensity (thickness of flood deposits) with (A) the  
971 Allos flood record from the southern French Alps (Wilhelm et al., 2012a), (C) the BAR flood  
972 record from the northern French Alps (Wilhelm et al., 2013) and (D) the tree-ring-based  
973 summer temperature for the European Alps (Büntgen et al., 2011). The reconstructed  
974 *Sporomiella*-type flux is also shown next to the Foréant flood record to highlight potential  
975 human impacts (i.e. grazing) on the erosion processes that might bias the flood record. The  
976 red stars below the Foréant record show the chronological markers with their 2-sigma  
977 uncertainty ranges.

## Supplementary Material

### **A millennium of flood activity at the climatic boundary between Atlantic and Mediterranean influences**

B. Wilhelm<sup>1,2</sup>, H. Vogel<sup>2</sup>, C. Crouzet<sup>3</sup>, D. Etienne<sup>4,5</sup>, F. Anselmetti<sup>2</sup>

<sup>1</sup>Univ. Grenoble Alpes, LTHE, F-38000 Grenoble, France

<sup>2</sup>Institute of Geological Sciences and Oeschger Centre for Climate Change Research, Univ. of Bern, CH-3012 Bern, Switzerland

<sup>3</sup>Univ. Savoie Mont Blanc, CNRS, ISTERre, F-73376 Le Bourget-du-Lac, France

<sup>4</sup>UMR INRA 42 CARTELE, Univ. Savoie Mont Blanc, F-73376 Le Bourget du Lac, France

<sup>5</sup>INRA, CARTELE, F-74200 Thonon-les-Bains, France

#### **Chronology: detailed methods for palaeomagnetic investigations**

Palaeomagnetic investigations were performed at the CEREGE laboratory (Aix-Marseille University) on cores FOR13P1, FOR13P2 and FOR13P4 using u-channels sub-samples. The natural remanent magnetization (NRM) was progressively demagnetized using alternating fields with 10, 20, 30, 40, 60, 80 and 100 mT steps. In order to distinguish different mineralogical and grain-size fractions within the magnetic components, two types of laboratory remanent magnetizations were conducted: Isothermal Remanent Magnetization (IRM) and Anhyseretic Remanent Magnetization (ARM). ARM was produced in-line along the u-channel axis, using a 100 mT alternating field with a superimposed 0.05 mT steady field. IRM was obtained by passing the u-channels through two different Halbach cylinders that develop fields of 1 and 0.3 T, respectively (Rochette et al., 2001). For ARM and IRM1T, demagnetization was done following steps of 10, 20, 30, 40, 60, 80 and 100 mT. The magnetizations have been measured before alternating-field treatment and after each step using the 3-axis 2-G enterprise cryogenic magnetometer located in a shielded room. Additionally, anisotropy of magnetic susceptibility has been measured using AGICO MFK1-FA Kappabridge (spinning specimen method) to control the preservation of the sedimentary

fabric. The susceptibility ellipsoid is defined by three eigenvectors ( $K_{max}$ ,  $K_{int}$  and  $K_{min}$ ). The magnetic fabric is usually comparable to the sediment fabric with inclination of the  $K_{min}$  close to the vertical (Borradaile, 1988; Rochette et al., 1992; Tarling and Hrouda, 1993).

| <b>Flood date</b>  | <b>Affected rivers</b>       | <b>Spatial extent of the flood</b> | <b>Victim</b> | <b>Damage</b> | <b>Disruptions</b> | <b>Details on the hydro-meteorological causes</b>                        |
|--------------------|------------------------------|------------------------------------|---------------|---------------|--------------------|--|
| > 3 September 2012 | Guil                         | Ristolas and villages downstream   | N             | Y             | Y                  | Easterlies winds with heavy rainfalls in the upper part of catchment     |
| 28 May 2008        | Guil                         | Ristolas and villages downstream   | Y             | Y             | Y                  | Heavy rainfall event   |
| 13 June 2002       | Torrents of Segure and other | Ristolas                           | N             | N             | N                  | Heavy rainfalls mainly in the upper part of the catchment                |
| > 15 July 2002     | Guil                         | Ristolas and villages downstream   | N             | Y             | Y                  | Easterlies winds with heavy rainfalls in the upper part of the catchment |
| > 15 October 2000  | Guil and other               | Ristolas and villages downstream   | N             | Y             | N                  | 5 days of heavy rainfalls with increased rainfall depths the last 2 days |
| 13 June 2000       | Guil and Torrent of Segure   | Ristolas and villages downstream   | N             | Y             | Y                  | Heavy rainfalls mainly in the upper part of the catchment                |
| > July 1992        | Torrent of Bouchouse         | Ristolas                           | N             | Y             | Y                  | Violent thunderstorms  |
| 11 June 1978       | Guil                         | Ristolas and villages downstream   | N             | Y             | U                  |  |
| 5 May 1973         | Guil                         | Ristolas and villages downstream   | N             | Y             | U                  |  |
| > 1 November 1963  | Undefined                    | Ristolas                           | N             | Y             | U                  |  |
| 21 May 1959        | Guil                         | Ristolas and villages downstream   | N             | Y             | Y                  |  |
| > Summer 1959      | Guil                         | Ristolas and villages downstream   | N             | U             | Y                  |  |
| 13 June 1957       | Guil and Torrent of Segure   | Ristolas and villages downstream   | N             | Y             | Y                  | Heavy rainfalls, thunderstorm, snowmelt                                  |
| > October 1953     | Torrent of Jalinette         | Ristolas                           | N             | Y             | Y                  | Heavy rainfall event   |
| > 29 Sept. 1953    | Guil                         | Ristolas and villages downstream   | N             | Y             | Y                  | Heavy rainfall event during 3 days                                       |
| > 1 July 1953      | Torrent of Jalinette         | Ristolas                           | N             | Y             | Y                  |  |
| 8 June 1953        | Guil                         | Ristolas and villages downstream   | N             | Y             | Y                  | Violent thunderstorms and snowmelt                                       |
| 14 May 1948        | Guil                         | Ristolas and villages downstream   | Y             | Y             | Y                  | Rainfall depth of 244 mm in 3 days, with snowmelt                        |
| > 4 August 1938    | Torrent of Segure            | Ristolas                           | N             | Y             | Y                  | Violent thunderstorms  |
| 1932               | Torrent of Maloqueste        | Ristolas                           | N             | Y             | U                  |  |
| > 9 July 1932      | Guil                         | Ristolas and villages downstream   | N             | Y             | Y                  |  |
| > 1 September 1920 | Guil                         | Ristolas and villages downstream   | N             | Y             | Y                  |  |
| 29 May 1856        | Guil                         | Ristolas and villages downstream   | N             | U             | U                  | Heavy rainfalls over a long period before the flood event                |
| > 6 August 1852    | Guil                         | Ristolas and villages downstream   | N             | Y             | Y                  | Heavy rainfall events  |
| > 15 October 1839  | Guil                         | Ristolas and villages downstream   | N             | Y             | U                  | Heavy rainfall events  |
| > 13 Sept. 1810    | Guil and Torrent of Segure   | Ristolas and villages downstream   | N             | Y             | Y                  | Heavy rainfall events during 8 days                                      |
| > 13 October 1810  | Guil                         | Ristolas and villages downstream   | N             | Y             | Y                  |  |
| > 10 October 1791  | Guil and Torrent of Chapelle | Ristolas and villages downstream   | N             | Y             | Y                  |  |
| > 9 October 1790   | Guil                         | Ristolas and villages downstream   | N             | Y             | Y                  |  |
| 1789               | Guil                         | Ristolas and villages downstream   | N             | Y             | Y                  |  |
| > 07 Sept. 1788    | Guil                         | Ristolas and villages downstream   | N             | Y             | Y                  |  |
| > 7 September 1787 | Guil                         | Ristolas and villages downstream   | N             | Y             | U                  |  |
| > 4 October 1751   | Guil                         | Ristolas and villages downstream   | N             | U             | U                  | Heavy rainfall events  |

**Table S1.** List of historical flood events which runs through the village of Ristolas, located 8 km downstream from Lake Foréant (from the free-access database of the ONF-RTM, <http://rtm-onf.ifn.fr/>). The arrows in the first row highlight the floods that occurred in summer and fall, i.e. that may be recorded in the lake sediments because this period corresponds to the ice-free season of Lake Foréant. N means No, Y means Yes and U, Uncertain.

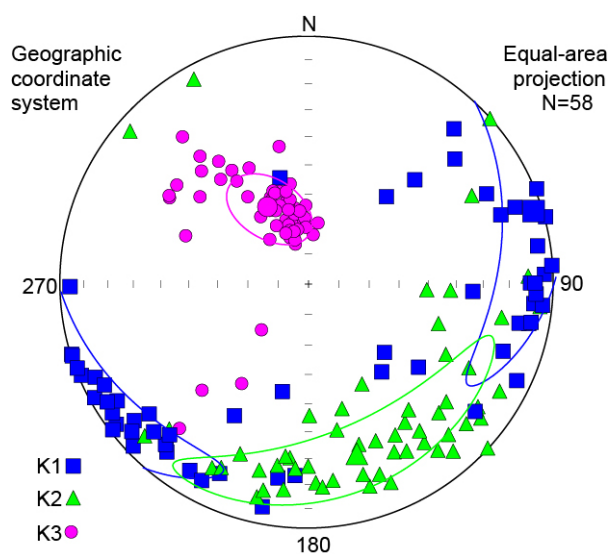


**Fig. S1.** Results of Anisotropy of Magnetic Susceptibility for core FOR13P4: stereo plot of the main axes direction. Notice that the K3 is well grouped and close to the vertical except some points associated with MMITs.

FOR13 P3 88 cm  
MAD = 2,17  
Units:  $2 \cdot 10^{-4}$  A/m

FOR13 P1 10 cm  
MAD = 1,67  
Unit:  $10^{-4}$  A/m

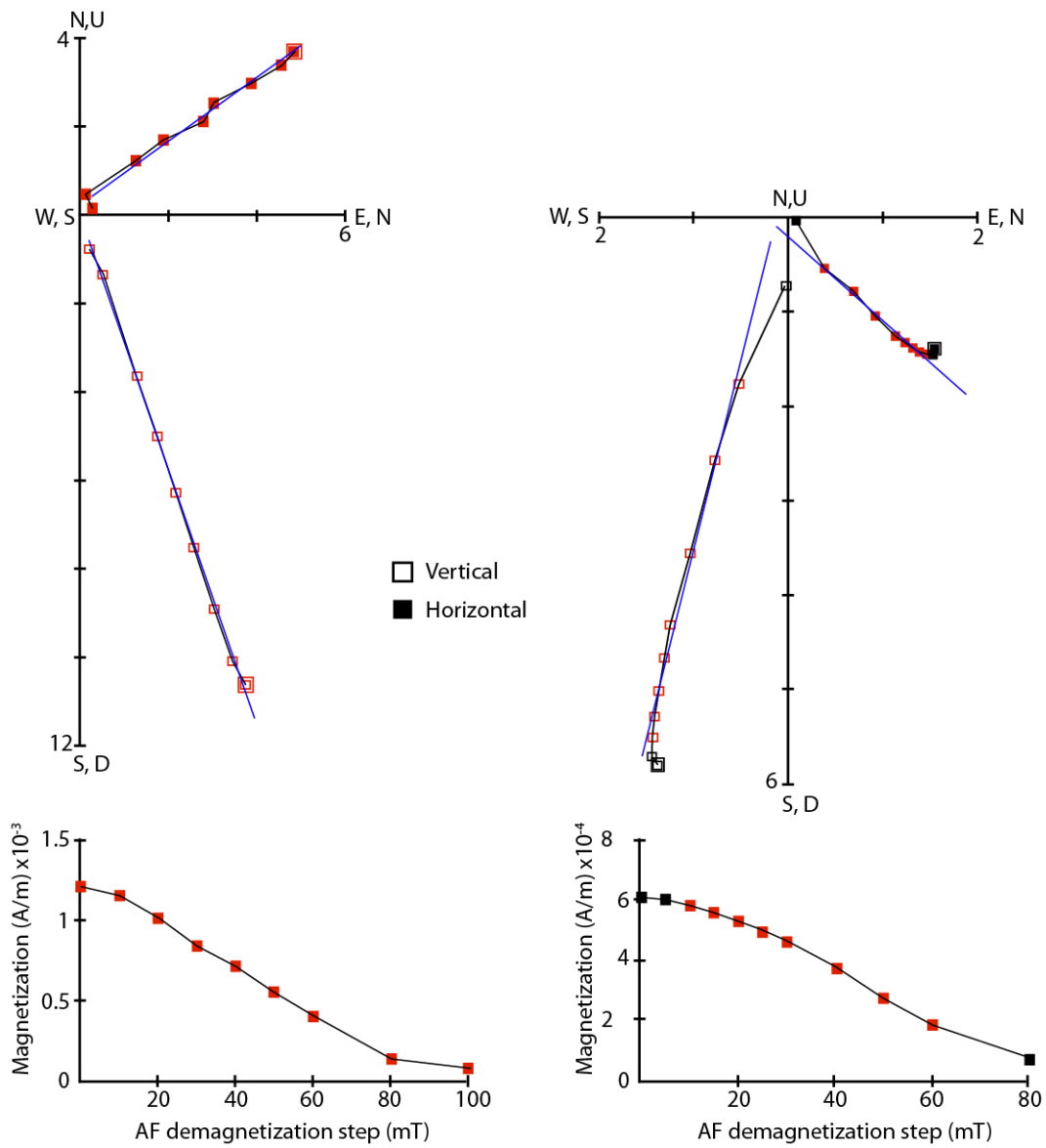


**Fig. S2.** Example of stepwise alternating field demagnetization of NRM (orthogonal vector projections and intensity curves) for representative samples. Solid (open) symbols are horizontal (vertical) plane projections.

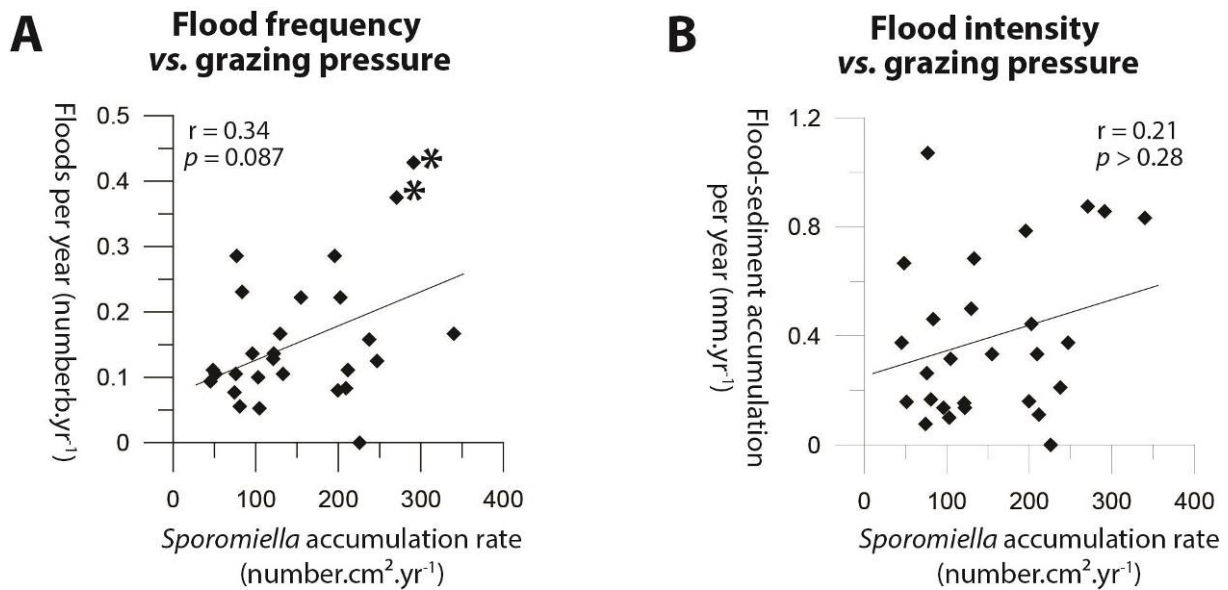


**Fig. S3.** Representation and correlation coefficients ( $r$ ) of relations between (A) *Sporormiella* accumulation rates (number.cm<sup>2</sup>.yr<sup>-1</sup>) and floods frequency (nb.yr<sup>-1</sup>), and between (B) *Sporormiella* accumulation rates (number.cm<sup>2</sup>.yr<sup>-1</sup>) and flood-sediment accumulation (mm.years<sup>-1</sup>). The stars identified two samples, dated from 1734 to 1760 AD, with both high grazing pressure and high flood frequency. Levels of significance ( $p$  values) were determined using a Spearman-test.

## References

- Rochette, P., Jackson, M., Aubourg, C.: Rock magnetism and the interpretation of anisotropy of magnetic susceptibility, *Reviews of Geophysics* 30 (3), 209–226, 1992.
- Rochette, P., Vadeboin, F., Clochard, L.: Rock magnetic applications of Halbach cylinders, *Physics of the Earth and Planetary Interiors* 126, 109–117, 2001.
- Borradaile, G.: Magnetic susceptibility, petrofabrics and strain, *Tectonophysics*, 156, 1–20, 1988.
- Tarling, D.H., Hrouda, F.: *The Magnetic Anisotropy of Rocks*, Chapman & Hall, London (218 pp.), 1993.